Analysis and simulation of K and Cl in electrostatic precipitator ash and black liquor of an operating kraft recovery boiler

by

Quinten Ilkka

A thesis presented to Lakehead University in fulfillment of the thesis requirement for the degree of Master of Science in Chemical Engineering

Thunder Bay, Ontario, Canada, 2023

Abstract

Non-process elements such as potassium (K) and chlorine (Cl) are commonly found in the recovery cycle of kraft mills and are capable of forming highly soluble compounds. These elements, in high concentrations, can lead to the corrosion of process equipment or to the plugging of recovery boilers. The behaviour of these elements throughout the liquor cycle is often a direct result of variables related to the operation of the process. An unusual cyclical trend was observed in the Cl content of the electrostatic precipitator (ESP) ash produced in the recovery boiler of a Canadian kraft mill. Analysis of the ash and liquor samples during a 390-day sampling period found that the Cl enrichment factor (EF_{Cl}) varied significantly between 1.2 to 3.9, whereas the EF_K stayed fairly constant at ~ 1.4.

The cyclical trend has a near annual period and was predictable over 5 years, with the exception of a single unusual 90-day duration. Investigation of available mill data and insight from mill personnel were unable to explain these trends. A literature investigation was conducted into process variables known to affect enrichment factors and recovery cycle concentrations: black liquor composition, black liquor dissolved solids content, amount of combustion air, lower furnace temperature, flue gas SO_2 concentration, amount of ESP ash purged, and grade of caustic used. Of these variables studied, none were able to explain the observed trends.

A model was developed using the CADSIM software to simulate the K and Cl in the recovery cycle and attempt to replicate the observed trends. It was validated by using available mill data, and it was effectively able to replicate the trend of K. A sensitivity analysis of the K input used in the model was also conducted. Results from this sensitivity analysis found that the model could reliably replicate the observed trend for a given K input by tuning the model. This model was

unable to reproduce the Cl trends in the mill data using a single constant EF_{Cl}. However, by using multiple EF_{Cl} values, a hypothetical trend was produced that agreed with the mill data.

A study was conducted in CADSIM to evaluate the effect of purging ESP ash on the concentrations of K and Cl in the liquor cycle. A simple mathematical model was devised to estimate K and Cl concentrations in the recovery cycle. Results from this mathematical model agreed with trends from the study. The times needed for K and Cl concentrations to reach steady-state values in the recovery cycle were determined to be different when purging ESP ash. The trends for the K and Cl concentrations in ESP ash at different purge flow rates were also predicted.

Acknowledgements

I want to thank my supervisor, Dr. Lionel Catalan, for the guidance, support, and valuable advice he provided throughout this thesis. His supervision allowed for an incredible opportunity to learn to critically think and to apply it when solving practical problems. I also would like to thank my co-supervisor, Dr. Pedram Fatehi, for his guidance. While our time spent together may have been limited, your guidance and thorough input provided was invaluable.

I am grateful for the financial support provided by the Dr. Joseph Swartz Memorial Scholarship and the Department of Chemical Engineering. I would like to thank the Resolute Forest Products Kraft Mill for providing me with the data and tools needed for this project. I would like to acknowledge Kyle Watkins, who helped clarify questions and provided his expertise and knowledge of the process at the Resolute Mill.

Finally, I would like to extend my thanks to all my friends and family for their encouragement and support during my studies.

Table of Contents

List of Tables

List of Figures

List of Appendices

1. Introduction

1.1 Kraft Pulping Process

The pulping process is the extracting or liberating of cellulose fibres (pulp), a linear β-glucose polymer, from the complex wood matrix. The wood matrix primarily consists of carbohydrates (cellulose and hemi-cellulose, highly branched polymers of several base sugars), extractives, and lignin. Extractives are a mixture of many species which are easily dissolved during the pulping process, and lignin is an amorphous highly branched large polymer derived from three base monomers: p-coumaryl alcohol, sinapyl alcohol, and coniferyl alcohol (Brännvall, 2009; Burazin, 1986; Chakar & Ragauskas, 2004; Koch, 2006).

The kraft, also known as sulfate, pulping process uses NaOH and Na_2S to dissolve the hemi-cellulose and lignin in the wood matrix. This dissolving is achieved by first breaking down the highly branched hemi-cellulose and large lignin polymers through chemical reactions, and then, by separating them from the mainly undissolved cellulose (pulp) fibres. The popularity of the kraft process is due to the excellent properties of its resulting pulp products, the range of raw materials it can be applied to, and its ability to regenerate the NaOH and Na_2S within the process (Andersson, 2014: Brännvall, 2009; Koch, 2006).

A flow diagram of a typical kraft pulping process can be seen in Figure 1.1. The process begins with wood, which is debarked, chopped into chips, and typically pre-treated with steam. The pre-treated wood is then mixed with a chemical solution consisting primarily of NaOH and Na_2S, called white liquor. The mixing and subsequent reactions, known as cooking, are carried out in a highly controlled vessel, known as a digester. The temperature, liquor concentration, and residence time inside the digester are controlled to ensure that the resulting pulp has the desired properties

and that the loss of pulp is minimized during the cooking process. As a result, it is important to monitor the Na and S concentrations at this point in the kraft process (Andersson, 2014; Gellerstedt, 2009).

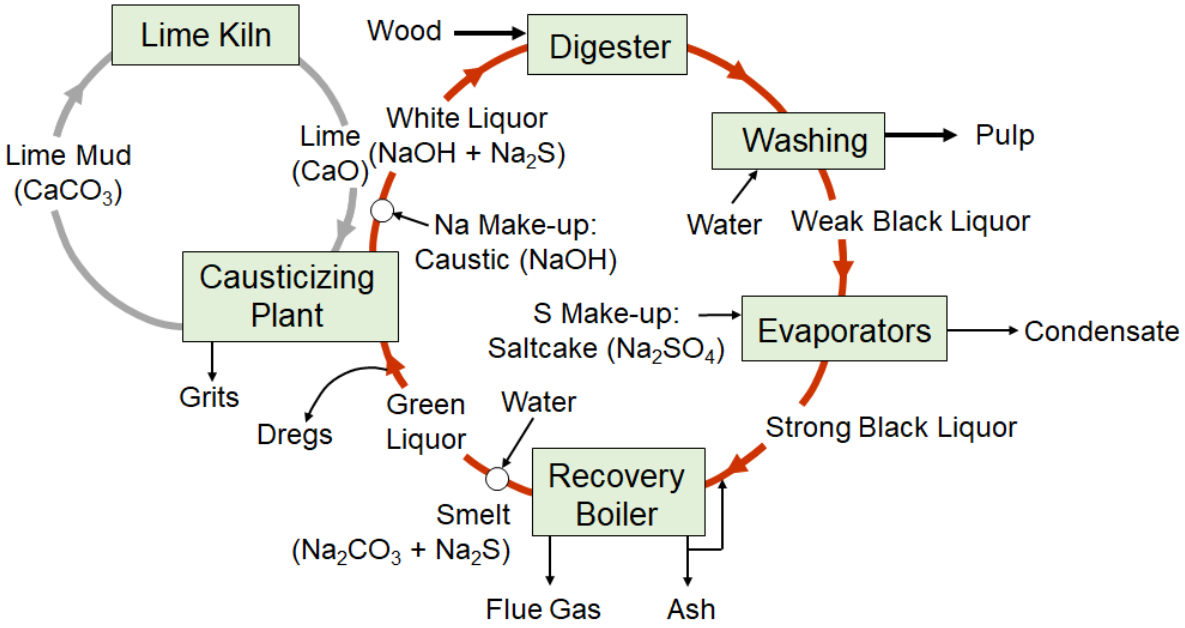

Figure 1.1: Flow diagram of a typical kraft pulping process.

The product pulp produced by the digester is separated from the remaining cooking solution, called black liquor, in a process known as washing. The washing process utilizes several methods such as displacement, dilution, extraction, or diffusion. A typical washing process consists of diluting the pulp slurry in a vessel and forming a layer, or mat, of pulp on a rotating drum attached to a vessel. The drum typically operates with some pressure gradient across the drum to assist in the extraction of the spent cooking solution through the pulp mat. A cleaning fluid, often water, is sprayed onto the mat to displace residual or entrained cooking solution in the pulp mat (Miliander, 2009; Santos & Hart, 2014).

The economic advantage of the kraft process comes from its ability to regenerate the chemicals needed for the cooking process. The first step of this regeneration is the concentration of the black liquor, which contains the used cooking chemicals and energy-dense dissolved organic materials. The black liquor which comes from the washing process has a low dissolved solids content (around 20 %) and is known as weak black liquor. This weak black liquor is concentrated in a series of evaporators (Figure 1.2) to produce strong black liquor containing a higher dissolved solids content (around 50%). At this point, the first make-up chemical is added generally in the form of saltcake (Na_2SO_4). The strong black liquor is then concentrated further (often times above 70%) to yield as-fired black liquor (Theliander, 2009a).

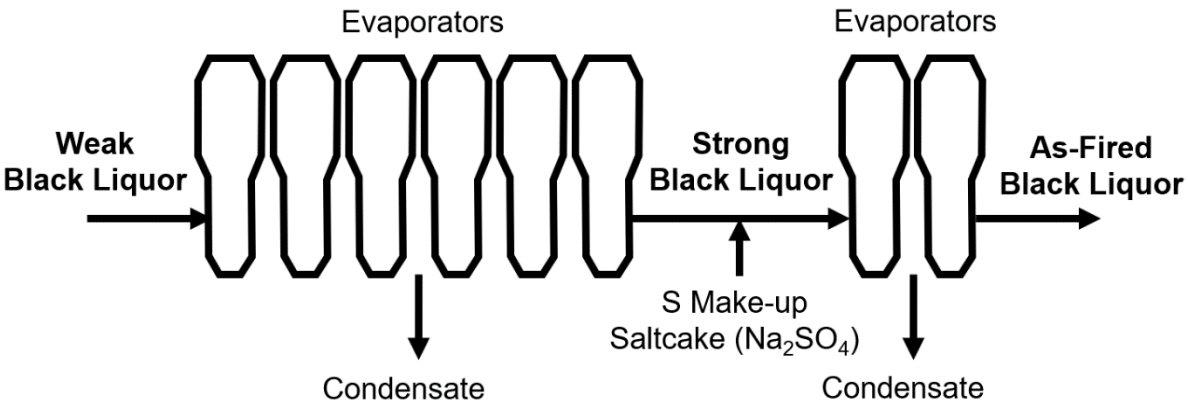

Figure 1.2: Flow diagram of a typical black liquor evaporation process.

The as-fired liquor is then combusted with additional air in a furnace, known as a recovery boiler (Figure 1.1), to extract the heat value of the dissolved organic materials and to reduce the Na_2SO_4 in the black liquor to Na_2S. This combustion process also produces hot flue gases that heat boiler feed water to produce high-pressure steam. The cooled flue gases are then released to the environment (Hupa, 2007; Theliander, 2009a).

The reduced cooking chemicals exiting the recovery boiler are a molten salt mixture, called smelt, consisting primarily of Na_2CO_3 which originates from the black liquor and Na_2S coming from the reduction of Na_2SO_4. The smelt is then mixed with water to form a solution known as green liquor. The Na_2CO_3 in the green liquor solution is converted into NaOH in a process known as causticizing. The causticizing process occurs by the addition of slaked lime ($Ca(OH)_2$) to the green liquor. This addition occurs in a vessel, called a slaker, and the reaction continues in additional vessels, called causticizers. The causticizing process produces an alkaline solution consisting primarily of the now regenerated NaOH and Na_2S, i.e., the main constituents of white liquor. Make-up NaOH, also called caustic, is added to the white liquor before entering the digester to maintain the concentrations needed for the cooking process. This process of using and regenerating the white liquor is referred to as the liquor cycle of the kraft pulping process (Henricson, 2005; Sanchez, 2007; Swanda et al., 1997; Theliander, 2009b).

A by-product of the causticizing process is lime mud ($CaCO_3$), an alkaline insoluble material which can easily be separated from the produced white liquor through filters. The separated lime mud is then decomposed in a kiln to regenerate the lime (CaO) needed for the causticizing process. This process of using and regenerating the lime is referred to as the lime cycle (Mehtonen, 2013; Sanchez, 2007; Theliander, 2009b; Tran, 2007a).

1.2 Recovery Boiler Operations

The function of the recovery boiler is to produce the Na_2S needed, to ensure the complete combustion of organic materials in the black liquor, and to recover most of the thermal energy subsequently produced from this combustion. The production of the desired species and complete combustion of the organic materials are achieved in the lower portion of the recovery boiler, known as the lower furnace. Here, black liquor is sprayed in the form of droplets, and air is injected at various levels of the lower furnace, which can be seen in Figure 1.3 (Henricson, 2005; Theliander, 2009a; Vakkilainen, 2006).

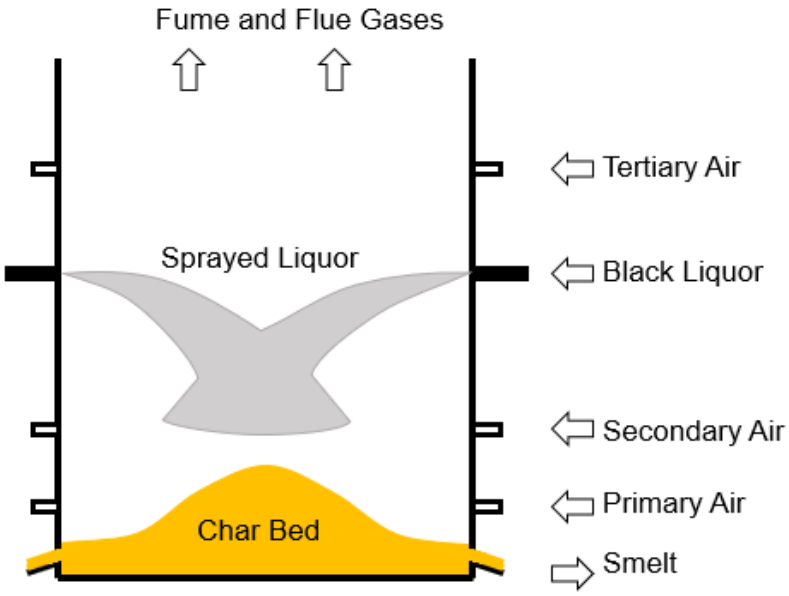

Figure 1.3: Flow diagram of the lower furnace of a kraft recovery boiler.

The black liquor is sprayed as droplets to ensure that the combustion process is completed before reaching the molten salt bed at the bottom of the recovery boiler, called a char bed. This in-flight combustion of the black liquor droplets consists of several stages: drying, devolatilization, and char burning. Drying is the evaporation of the water from the droplet. Devolatilization involves

the pyrolysis – another name for this stage – of the organic matter and burning of volatile gases in the droplet; this process causes the droplet to swell significantly. The final stage is char burning. Here, carbon is burned from the surface of the droplet, and the size of the droplet is reduced significantly. Once the droplet reaches the char bed, further reactions occur to cycle the sulfur in the char bed between Na_2SO_4 and the desired Na_2S (Reactions 1.1 to 1.3). The molar ratio of Na_2S to the sum of all sulfur species in the produced smelt is called the reduction efficiency of the recovery boiler. Modern recovery boilers typically achieve reduction efficiencies greater than 90% (Hupa, 2007; Hupa & Frederick, 2007; Theliander, 2009a, Vakkilainen, 2006).

$$Na_2S_{(l)} + 2O_{2(g)} \rightarrow Na_2SO_{4(l)} \qquad \textbf{(Rxn 1.1)}$$

$$Na_2SO_{4(l)} + 4C \rightarrow Na_2S_{(l)} + 4CO_{(g)} \qquad \textbf{(Rxn 1.2)}$$

$$Na_2SO_{4(l)} + 2C \rightarrow Na_2S_{(l)} + 4CO_{2(g)} \qquad \textbf{(Rxn 1.3)}$$

Tertiary air enters the furnace above the sprayed liquor to create an oxygen rich environment needed for the combustion of organic vapors and suspended matter in the rising flue gases. In contrast, the amount of air entering above the char bed (primary and secondary air) is limited to still combust the liquor droplets but also to create an oxygen deficient environment desirable for the reduction reactions (Reactions 1.2 and 1.3) needed on the surface of the char bed (Theliander, 2009a; Vakkilainen, 2006).

In addition to the reduction reactions on the surface of the char bed, several other reactions can occur which change the composition of the char bed (Reactions 1.4 and 1.5). It is important to note that while these reactions do occur in the char bed, their extent is quite small. Hence, relatively low amounts of NaOH are produced in the smelt, and the large amounts of Na_2CO_3 present in the produced smelt come almost entirely from the black liquor (Vakkilainen, 2006).

$$Na_2CO_{3(l)} + H_2O_{(g)} \rightarrow 2NaOH_{(l)} + CO_{2(g)} \quad \textbf{(Rxn 1.4)}$$

$$Na_2S_{(l)} + CO_{2(g)} + H_2O_{(g)} \rightarrow Na_2CO_{3(l)} + H_2S_{(g)} \quad \textbf{(Rxn 1.5)}$$

Some reactions release species and compounds directly from the char bed, as shown in Reactions 1.6 and 1.7. The release of NaCl from the char bed into the flue gas (Reaction 1.7) is the sole mechanism for Cl release into the gas phase. It is also important to note that while all of the reactions have been shown for Na compounds for simplicity, similar reactions occur for K equivalent compounds (Vakkilainen, 2006).

$$Na_{(l)} \rightarrow Na_{(g)} \quad \textbf{(Rxn 1.6)}$$

$$NaCl_{(l)} \rightarrow NaCl_{(g)} \quad \textbf{(Rxn 1.7)}$$

The Na and NaCl gas species react with water vapors to form sodium hydroxide in the gas phase, as shown in Reactions 1.8 and 1.9 (Jokiniemi et al., 1996; Vakkilainen, 2006).

$$Na_{(g)} + H_2O_{(g)} \rightarrow NaOH_{(g)} + \frac{1}{2}H_{2(g)} \quad \textbf{(Rxn 1.8)}$$

$$NaCl_{(g)} + H_2O_{(g)} \rightleftarrows HCl_{(g)} + NaOH_{(g)} \quad \textbf{(Rxn 1.9)}$$

As the flue gas leaves the lower furnace and begins to cool, the metallic compounds quickly begin to condense onto seed particles present in the furnace (Reactions 1.10 to 1.13), where the subscript c denotes the condensed phase. The condensation of these metallic compounds form submicron particles, known as fume, which travel with the flue gas through the recovery boiler (Jokiniemi et al., 1996).

$$NaCl_{(g)} \rightarrow NaCl_{(c)} \quad \textbf{(Rxn 1.10)}$$

$$NaOH_{(g)} + CO_{2(g)} \rightarrow NaOH_{(c)} + CO_{2(g)} \quad \textbf{(Rxn 1.11)}$$

$$2NaOH_{(g)} + SO_{2_{(g)}} + \frac{1}{2}O_{2_{(g)}} \rightarrow Na_2SO_{4_{(c)}} + H_2O_{(g)} \qquad \textbf{(Rxn 1.12)}$$

$$2NaOH_{(g)} + CO_{2_{(g)}} \rightarrow Na_2CO_{3_{(c)}} + H_2O_{(g)} \qquad \textbf{(Rxn 1.13)}$$

The composition of these fume particles can change as they react with various species present in the flue gas, as shown in Reactions 1.14 to 1.16 (Jokiniemi et al., 1996; Tran & Earl, 2004).

$$2NaCl_{(c)} + SO_{2_{(g)}} + \frac{1}{2}O_{2_{(g)}} + H_2O_{(g)} \rightarrow Na_2SO_{4_{(c)}} + 2HCl_{(g)} \qquad \textbf{(Rxn 1.14)}$$

$$2NaOH_{(c)} + SO_{2_{(g)}} + \frac{1}{2}O_{2_{(g)}} \rightarrow Na_2SO_{4_{(c)}} + H_2O_{(g)} \qquad \textbf{(Rxn 1.15)}$$

$$2NaOH_{(c)} + CO_{2_{(g)}} \rightarrow Na_2CO_{3_{(c)}} + H_2O_{(g)} \qquad \textbf{(Rxn 1.16)}$$

The reactions previously shown are only the main of many reactions occurring in the recovery boiler, which demonstrates how complex the recovery boiler system is.

In addition to fume particles which travel with the flue gas along the recovery boiler, there are other particles which also become entrained in the flue gas. The first and largest of these particles are a result of the black liquor droplets being sprayed into the recovery boiler, which can be seen in Figure 1.4. The ideal droplet size is one which reaches the char bed while still char burning. If the droplets are too big, they fall too quickly and reach the char bed still wet. This leads to a lower temperature of the char bed, resulting in adverse effects such as an increase in the amount of SO_2 released, which is undesirable. If the droplets are too small, however, they can become completely entrained in the upward flow of flue gas, known as carryover particles. These droplets can alternatively become trapped initially in the upward flow of flue gas as the droplets expand during the pyrolysis phase, but then fall to the char bed later as the droplet size decreases during the char

burning phase. This is also undesirable as the droplet reaches the char bed oxidized, and results in a lower reduction efficiency of the recovery boiler, which is also undesirable (Brink, 2021; Theliander, 2009a; Wessel, 2007).

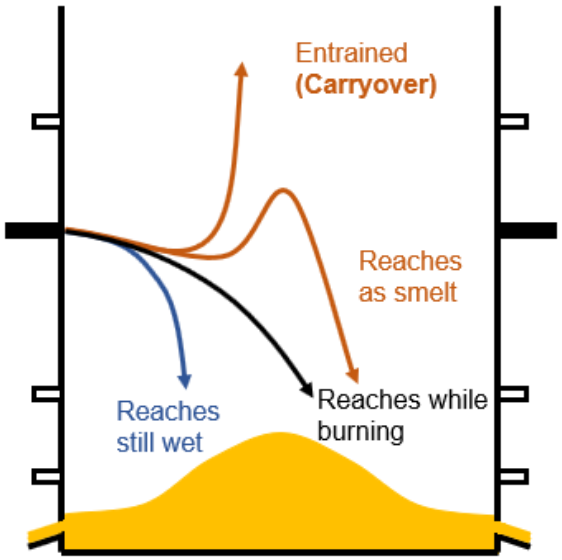

Figure 1.4: Trajectories of sprayed black liquor droplets.

The other particle type present in the flue gas is a consequence of the black liquor combustion. During the pyrolysis phase, the volatile gases of droplet expand and release from the droplet. As the gas within the droplet expands, small amounts of the droplet are ejected and become entrained in the flue gas. These particles, called intermediate sized particles or ejecta, are larger than resulting fume particles but are smaller than carryover particles (Khalaj-Zadeh, 2008; Kochesfahani, 1999; Tran, 2007b; Wessel et al., 2004; Vakkilainen, 2006).

In order to recover the thermal energy produced from the combustion of the organic material of the black liquor, the flue gas passes through a series of several banks of tubes in the upper furnace, as shown in Figure 1.5. The first of these heat transfer sections, superheaters, occurs when the flue gas is hottest and produces super heated steam. In the next section, called the generating or boiler

bank, saturated steam is generated from saturated boiler feed water. In the final section, known as the economizers, boiler feed water is heated to its saturation temperature (Henricson, 2005; Theliander, 2009a; Vakkilainen, 2006).

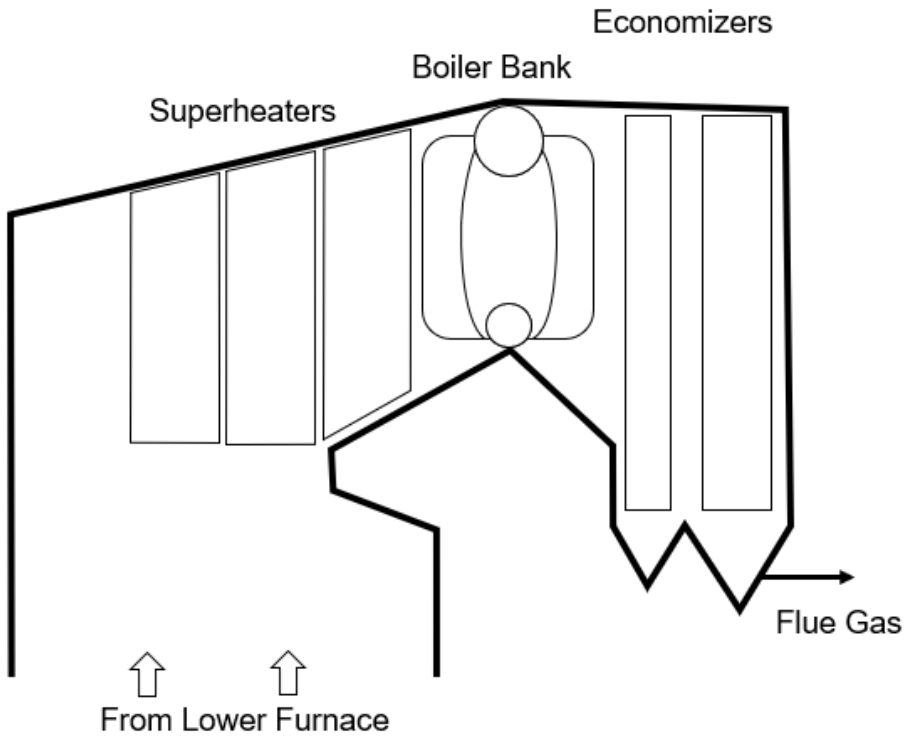

Figure 1.5: Flow diagram of the upper furnace of a kraft recovery boiler.

Groups of tubes in each section of the upper furnace are tightly packed and are often represented as a single heat transfer surface; these banks of tubes are spaced accordingly based on their position in the upper furnace. Banks of tubes in the superheater sections are widely spaced (300 – 400 mm) relative to the other sections such as the generating bank (250 – 150 mm) or the economizers (150 – 100 mm). This is because as the flue gas cools, particles travelling with the flue gas adhere to the cool heat transfer surfaces forming deposits. If left uncontrolled, these deposits can accumulate to the point of decreasing the thermal recovery efficiency. Even worse, they can cause a complete

blockage of flue gas passages, which is known as the plugging of the recovery boiler (Tran, 1986; Tran, 2007b; Vakkilainen, 2006).

The composition of these deposits can vary across recovery boilers and liquors resulting from different species of pulp. However, in general there are several important phases and corresponding temperatures that occur as a deposit melts. The first of these, the first melting temperature, occurs when the solid deposit begins to melt or liquid first appears in the deposit. Next, the sticky temperature is the point at which the liquid fraction of the deposit reaches 15%; here, the rate of deposition of a deposit begins to accumulate rapidly. After this, the phase known as the slagging or radical deformation temperature happens once the liquid fraction of the deposit reaches 70%. At this point, the deposit begins to fall from the heat transfer surface under its own weight, and the rate of deposition of a deposit ceases. Lastly, the complete melting temperature occurs when the deposit is fully melted (Isaak et al., 1986; Tran, 2007b).

The region of a recovery boiler which operates between the sticky and slagging temperatures is known as the sticky region; this operating range is the area where deposits are likely to form. A recovery boiler is said to be plugged when the sticky region of a recovery boiler extends into the generating bank. This is because the superheater sections are designed with large spaces between the banks of tubes to account for the deposits which will form. In contrast, the generating bank is not designed to have these large deposits form, and consequently, the flue gas passages can easily become blocked (Isaak et al., 1986; Tran, 1986; Tran, 2007b).

Deposits form on the heat transfer surfaces by various methods. Large particles entrained in the flue gas, such as carryover and ejecta, form deposits from the inertial impact on the heat transfer surfaces. Deposits that form in the superheaters are generally dominated by this mechanism. These deposits tend to be quite hard and difficult to remove effectively by soot blowers and often require

shutdowns of the recovery boiler to do so. Smaller particles, such as fume, form deposits by the temperature gradient between the hot particles and cool heat transfer surface in a process known as thermophoresis. Also, as the flue gas is cooling, metallic compounds still in the gas phase, such as NaCl, can form deposits by directly condensing on the cool heat transfer surfaces. Deposits formed by these mechanisms, which largely occur in the generating bank and economizers, are often brittle and dust like; they tend to be easily and effectively removed with soot blowers (Leppänen et al., 2014; Tran, 1986; Tran, 2007b; Vakkilainen, 2006).

After the flue gas exits the recovery boiler, it passes through an electrostatic precipitator (ESP). The purpose of this ESP is to separate and collect and any particles (carryover, ejecta, fume, etc.), collectively known as ash, which may still be entrained in the flue gas. This collected ash contains significant amount of cooking chemicals (Na and S). As a result, the ash is often partially purged or treated to separate the cooking chemicals before being recycled and mixed with as-fired liquor (Jones et al., 2015; Theliander, 2009a; Vakkilainen, 2006).

1.3 Causticizing Operations

As smelt dissolves in water to form green liquor, alkaline insoluble precipitates, known as dregs, form. The dominant mineral phase of these dregs is generally pirssonite ($Na_2CO_3 \cdot CaCO_3 \cdot 2H_2O$) or calcite ($CaCO_3$); however, the composition can differ from mill to mill based on differences throughout the pulping process. The dregs are filtered and purged from the green liquor prior to the causticizing process (Mäkitalo et al., 2014; Manskinen et al., 2010; Quina & Pinheiro, 2020; Taylor & McGuffie, 2007; Theliander, 2009b).

Once the green liquor has been clarified of the dregs, it enters a reactor, known as a slaker, where the green liquor is mixed with slaked lime ($Ca(OH)_2$). This slaked lime reacts with the Na_2CO_3 in the green liquor to create the desired NaOH by the causticizing reaction, as shown in Reaction 1.17 (Sanchez, 2007; Theliander, 2009b).

$$Na_2CO_{3(aq)} + Ca(OH)_{2(s)} \rightleftarrows 2NaOH_{(aq)} + CaCO_{3(s)} \qquad \textbf{(Rxn 1.17)}$$

The mixing of the green liquor and lime creates other alkaline insoluble precipitates, known as grits, which are again separated and purged. The dominant mineral phases of grits are generally found to be pirssonite, calcite, and larnite (Ca_2SiO_4) (Quina & Pinheiro, 2020; Martins et al., 2007; Theliander, 2009b).

Once the grits have been removed, the solution leaves the slaker and enters a series of agitated vessels, known as causticizers, to allow time for the causticizing reaction to reach near completion. Next, the generated lime mud ($CaCO_3$) by-product, which is insoluble in the white liquor solution, is filtered and separated from the white liquor (Henricson, 2005; Sanchez, 2007; Theliander, 2009b; Swanda et al., 1997).

The extent of the causticizing reaction is expressed as the ratio of the amount of NaOH produced, relative to the amount of NaOH produced and Na_2CO_3 initially present. This ratio is known as the causticizing efficiency (CE) and is shown in Equation 1.1. The amount of NaOH which is produced is generally expressed as the difference of NaOH concentrations in the white and green liquors (Sanchez, 2007; Swanda et al., 1997).

$$CE\ (\%) = \frac{([NaOH]_{WL} - [NaOH]_{GL})}{([NaOH]_{WL} - [NaOH]_{GL}) + [Na_2CO_3]_{WL}} \times 100\% \qquad \textbf{(Eq 1.1)}$$

The separated lime mud is decomposed in a kiln to regenerate lime (CaO) needed for the causticizing process, as shown in Reaction 1.18. The regenerated hot lime from the kiln is stored in a silo and brought via screw to the slaker. Here, the lime is slaked with water to produce the slaked lime needed for the causticizing process, as shown in Reaction 1.19 (Mehtonen, 2013; Sanchez, 2007; Theliander, 2009b; Tran, 2007a).

$$CaCO_{3_{(s)}} \rightarrow CaO_{(s)} + CO_{2_{(g)}} \qquad \textbf{(Rxn 1.18)}$$

$$CaO_{(s)} + H_2O_{(aq)} \rightarrow Ca(OH)_{2_{(s)}} \qquad \textbf{(Rxn 1.19)}$$

Since the concentrations of the white liquor impact the properties of the resulting pulp produced, it is important to monitor and control the white liquor concentrations. Some of the main properties of the white liquor which are monitored and controlled include the total titratable alkali (TTA), active alkali (AA), and sulfidity. The TTA of a liquor is the sum of the NaOH, Na_2CO_3, and Na_2S concentrations of the liquor, as shown in Equation 1.2. The AA of a liquor is the sum of the concentrations of the alkali species active in the cooking process (NaOH and Na_2S), as shown in Equation 1.3. Lastly, the sulfidity of a liquor is expressed as a ratio of Na_2S concentration to either the TTA or AA, as shown in Equation 1.4 for AA. The concentrations used in the equations of this

section (Equations 1.1 to 1.4) are generally expressed in terms of Na_2O (i.e., g Na_2O/L or lb_m Na_2O/ft^3) or, in some regions of the world, in terms of NaOH (Sanchez, 2007; Swanda et al., 1997).

$$TTA = [NaOH] + [Na_2CO_3] + [Na_2S] \quad \textbf{(Eq 1.2)}$$

$$AA = [NaOH] + [Na_2S] \quad \textbf{(Eq 1.3)}$$

$$Sulfidity\ (\%) = \frac{[Na_2S]}{AA} \times 100\% \quad \textbf{(Eq 1.4)}$$

1.4 Non-Process Elements

Non-process elements (NPEs) are defined as elements which do not actively participate in the kraft pulping process. These typically include any elements which are not Na, S, C, O, and H. It is important to note that different areas within the kraft process, such as causticizing operations, may define other species as NPEs (Karlemo, 2019; Manskinen et al., 2010; Mehtonen, 2013; Svensson, 2012; Tran & Vakkilainen, 2007).

The largest source of NPEs to the liquor cycle is wood, which contains over 70 NPEs that enter the liquor cycle. Other sources of NPEs to the liquor cycle include process water and make-up materials, such as caustic and saltcake (Karlemo, 2019; Manskinen et al., 2010; Ulmgren, 1997).

NPEs have been reported to cause significant problems for kraft mills. Some of these problems include additional capital expenses associated with the replacement of corroded equipment or additional operational costs associated with an increase of dead loads in certain areas of the mill, such as in the lime cycle. Other problems which can occur are additional process shutdowns to remove deposits or clear plugged recovery boilers (Bialik et al., 2015; Salmenoja et al., 2009; Ulmgren, 1997).

Not all NPEs are detrimental to mill operation, as most of them are removed before they reach large enough concentrations where issues can arise. The ability of a NPE to be able to accumulate to large enough concentrations in the liquor cycle is a direct result of its ability to form compounds which are soluble in the alkaline liquor solutions. Of NPEs observed in kraft mills, elements which are capable of forming such compounds include K, Cl, Si, and Al. Of these elements, K and Cl are the main NPEs monitored by mills, as they tend to enter the liquor cycle with higher concentrations. They are also the elements typically responsible for the more detrimental expenses

a mill can incur, such as the corroding of process equipment and plugging of the recovery boiler (Svensson, 2012; Ulmgren, 1997).

As mentioned previously, most NPEs leave the liquor at points in the liquor cycle where streams are naturally purged, such as ESP ash, dregs, and grits. The large amount of NPEs which do not form alkaline soluble compounds are easily removed from the liquor cycle by the dregs and grits, since they are precipitates of the alkaline liquor solutions. While K, Cl, Si, and Al can form alkaline soluble compounds, not all compounds formed are alkali soluble. As a result, even these species can be found in the dregs and grits. Although some K and Cl is purged with the dregs and grits, the resulting concentrations of K and Cl are still larger than ideal operating concentrations. K and Cl are, however, found to be concentrated in the ESP ash. Purging of this ash can, consequently, allow mills to operate at a lower (and more ideal) K and Cl concentration (Karlemo, 2019; Pfromm, 1999; Svensson, 2012; Ulmgren, 1997).

Values of K and Cl are typically reported as a molar ratio relative to the main cations present in the liquor (Na and K), as shown in Equation 1.5. This representation of the concentration allows for clear comparisons to be made at various locations within the liquor cycle and between data from different mills (Tran et al., 1990).

$$molar\ ratio = \frac{[Cl]\ or\ [K]}{[Na]+[K]} \qquad \textbf{(Eq 1.5)}$$

Additionally, values of K and Cl in streams can also be reported in a molar ratio relative to their concentration in the black liquor, known as an enrichment factor (EF), which can be seen in Equations 1.6 and 1.7 for K and Cl in ESP ash, respectively.

$$EF_K = \left(\frac{[K]}{[Na]+[K]}\right)_{ash} \Big/ \left(\frac{[K]}{[Na]+[K]}\right)_{liq} \qquad \textbf{(Eq 1.6)}$$

$$EF_{Cl} = \left(\frac{[Cl]}{[Na]+[K]}\right)_{ash} \Big/ \left(\frac{[Cl]}{[Na]+[K]}\right)_{liq} \quad \textbf{(Eq 1.7)}$$

Reported enrichment factors of ESP ash in literature are commonly around 1.5 for K and 2.5 for Cl, and typically assumed to be constant for a consistently operated recovery boiler (Jones et al., 2015; Tran et al., 1990).

1.5 Make-up Chemicals

1.5.1 Saltcake

The source of S make-up in the kraft process comes from Na_2SO_4, or saltcake, that is added to liquor cycle prior to the recovery boiler. Na_2SO_4 can be readily generated by mills as it is a by-product of a ClO_2 generation, a chemical commonly used in the downstream processing of pulp known as bleaching. The generation of ClO_2 is always done on-site due to the decomposition risk of ClO_2 and is generally produced from a sodium chlorate ($NaClO_3$) solution (Deshwal & Lee, 2005).

There are many ways in which ClO_2 is commonly generated from $NaClO_3$, however, most methods produce some form of saltcake as a by-product. One of the most common methods uses methanol and sulfuric acid to generate ClO_2 and is known as the R8 process shown in Reaction 1.22 (Deshwal & Lee, 2005; Saturnino, 2012).

$$6NaClO_3 + CH_3OH + 4H_2SO_4 \rightarrow 6ClO_2 + CO_2 + 2Na_3H(SO_4)_2 + 5H_2O$$

(Rxn 1.22)

The saltcake produced by this process is known as sodium sesquisulfate ($Na_3H(SO_4)_2$) and can be decomposed by metathesis to create a neutral saltcake shown in Reaction 1.23. This additional step of creating a neutral saltcake, when coupled with the R8 process, is known as the R10 process (ERCO Worldwide, n.d.; Öhman & Delin, 2014).

$$2Na_3H(SO_4)_2 \rightarrow 3Na_2SO_4 + H_2SO_4 \qquad \textbf{(Rxn 1.23)}$$

Another common method of ClO_2 generation from $NaClO_3$ uses hydrogen peroxide and sulfuric acid known as the R11 process shown in Reaction 1.24 (Deshwal & Lee, 2005; ERCO Worldwide, n.d.).

$$2NaClO_3 + H_2O_2 + H_2SO_4 \rightarrow 2ClO_2 + O_2 + Na_2SO_4 + 2H_2O$$

(Rxn 1.22)

1.5.2 Caustic

The additional source of Na make-up (and control of TTA in the white liquor) comes from the addition of a NaOH solution to the white liquor. Unlike saltcake, it is not generated on-site, but is purchased usually as a 50% solution by mass. This caustic solution can be used in other areas of the mill, such as in the bleaching process.

These caustic solutions are created from the electrolysis of NaCl solution in an electrolytic cell. There are two grades of caustic commonly used in the pulp and paper industry: diaphragm and membrane grade, which correspond to the type of electrolytic cell used in the electrolysis process (OxyChem, 2022).

The differences between these two grades of caustic are the amounts of starting materials (NaCl) present in the final caustic product, ultimately contributing additional Cl input to the liquor cycle. Diaphragm grade caustics typically contain around 1% NaCl by mass, whereas membrane grade caustics often only contain around 100 ppm NaCl (Old World Industries, LLC, 2016; OxyChem, 2022; Westlake Chemicals, 2022).

1.6 The Resolute Mill

The Resolute mill is a modern pulp mill located in Thunder Bay, Canada that first opened in 1924 and is capable of producing 554,000 tons of newsprint and market pulp annually. The mill produces kraft pulp products from an alternating source of hard and softwood materials. The mill also produces thermomechanical pulp (TMP) from recycled pulp materials. There are two paper machines in the mill that produce newsprint. The bleaching done by the mill is elemental chloride free (ECF) using chlorine dioxide generated from the R10 and R11 processes. The mill has one recovery boiler as well as a separate boiler for power generation that burns the non-condensable gases (NCG) (Resolute Forest Products, n.d.).

1.7 CADSIM Plus

CADSIM Plus is a chemical process simulation software developed by Aurel Systems. It is capable of performing mass and energy balances as well as simulating dynamic conditions. CADSIM also has many packages and modules designed for the pulp and paper industry, which is one of the many reasons that it is commonly used in this industry (Aurel Systems, n.d.).

1.8 Objectives

The purpose of this work is to:

1) Investigate an unusual trend observed over a long period of time in the Cl concentration of ESP ash of an operating kraft recovery boiler.
2) Create a simulation model of NPEs (K and Cl) in the liquor recovery cycle over time of a kraft mill.

The model was created in CADSIM and made for the Resolute mill using available data as input for the model.

2. Literature Survey

2.1 Enrichment Factors

The topic of enrichment factors, specifically of EF_K and EF_{Cl} in ESP ash, have been a significant topic in research for many years now. This is a result of the detrimental effects which K and Cl can have on mill operations, such as the plugging of recovery boilers. Changes in process variables can have a significant impact on resulting enrichments factors, which in turn affects the dynamics of mill operating strategies. The variables which have been studied include: black liquor composition, black liquor solids content, the amount of combustion air used, the temperature of the lower furnace, and the concentration of SO_2 in flue gas.

2.1.1 Black Liquor Composition

The effect of black liquor composition on enrichment factors was studied by Saturnino (2012). In his work, a model which used mass balances and a chemical equilibrium software was developed to predict the enrichment factors of ESP ash. During the testing of this model, the effect of the lower furnace temperature on enrichment factors was studied at various black liquor compositions. No clear nor significant trends were observed when changes were made to the Cl and K compositions in the black liquor. It was reported that properties of black liquor, which affect the composition of the ash, differed from one liquor to another; however, the influence these properties have on the sub-mechanisms that form ash is currently not clear.

2.1.2 Black Liquor Solids Content

The effect of the dissolved solids content of fired black liquor on enrichment factors was studied by Vakkilainen (2010). In his work, a model was developed to predict the enrichment factors of ESP ash as a function of fired black liquor dissolved solids content based on the analysis results from over 200 samples of ESP ash and black liquor. The model predicted that at dissolved solid contents greater than 70%, the EF_K consistently decreased gradually as the solids content increased. In contrast, the EF_{Cl} decreased significantly up to very high solid contents (around 85%), after which, the EF_{Cl} no longer changed as the solids content increased. The trend of this model was consistent with data from literature.

2.1.3 Amount of Combustion Air

The effect of the amount of combustion air on enrichment factors was studied by Saturnino (2012). During the testing of his model, as previously mentioned, the effect of the amount of combustion air was studied. It was found that there was a negligible change in the EF_K but a significant increase in the EF_{Cl} over the range studied.

The author reported that this observed trend was a result of the decrease in the amount of Na vapor released from the char bed, relative to the nearly constant amount of NaCl which is released. Due to the similarities of K and Na, nearly identical trends were also observed for K and KCl, which resulted in the constant EF_K observed. As the amount of oxygen increased, the subsequent decrease in the amount of Na and K vapor released (and ultimately Na and K in the ESP ash) caused the increase of the EF_{Cl}. This can be seen in the previously shown Equation 1.7 for lower amounts of Na and K in the ESP ash.

$$EF_{Cl} = \left(\frac{[Cl]}{[\boldsymbol{Na}]+[\boldsymbol{K}]}\right)_{ash} \Big/ \left(\frac{[Cl]}{[Na]+[K]}\right)_{liq} \qquad \textbf{(Eq 1.7)}$$

While the results from this model are valuable, one assumption of the model included that the temperature of the recovery boiler is independent of the amount of combustion air, which may not be representative of actual boiler operations.

2.1.4 Lower Furnace Temperature

The effect of the lower furnace temperature on enrichment factors was studied by Frederick et al. (1998) and Saturnino (2012). In the work by Frederick et al. (1998), experiments were run in a Laminar Entrained-Flow Reactor (LEFR) in which particles of black liquor solids were combusted at various temperatures, and the resulting enrichment factors were determined. Results from these experiments were combined with data from operating recovery boilers to predict the effect of lower furnace temperature on Cl enrichment factors. In the testing of Saturnino's (2012) model, as previously mentioned, it was found that EF_{Cl} and EF_K produce bell shaped trends with respect to lower furnace temperature. This bell shape of the EF_{Cl} trend matches the shape predicted by Frederick et al. (1998).

Frederick et al. (1998) reports that the bell shape observed for EF_{Cl} is a result of competing processes. At temperatures below the observed maximum of this trend, the amount of SO_2 produced is large enough to convert Cl in the ash into HCl in the flue gas, as shown previously in Reaction 1.14. At temperatures above the observed maximum of this trend, the increase in the amount of Na released into the gas phase (and ultimately Na in the ESP ash) is large enough to "dilute" the amount of Cl in the ash. This can be represented in the previously shown Equation 1.7 for higher amounts of Na in the ESP ash (Hupa, 2007).

$$2NaCl_{(c)} + SO_{2(g)} + \frac{1}{2}O_{2(g)} + H_2O_{(g)} \rightarrow Na_2SO_{4(c)} + 2HCl_{(g)}$$

(Rxn 1.14)

$$EF_{Cl} = \left(\frac{[Cl]}{[\boldsymbol{Na}]+[K]}\right)_{ash} \Big/ \left(\frac{[Cl]}{[Na]+[K]}\right)_{liq}$$ **(Eq 1.7)**

2.1.5 Flue Gas SO_2 Concentration

The effect of SO_2 concentration in the flue gas on enrichment factors was studied by Frederick et al. (1998). In this work, sets of experiments were run at several concentration of SO_2 in the flue gas. Results from these experiments were combined with data from Reis et al. (1995), which ran experiments in a similar LEFR without SO_2. Results from these experiments showed a decrease in EF_{Cl} as the SO_2 concentration increased; meanwhile, no noticeable nor significant trend was observed for EF_K.

The trend observed for the EF_{Cl} is a result of the additional SO_2 converting Cl, which otherwise would end up in the ash, into HCl in the flue gas, as previously shown in Reaction 1.14. The effect this has on the EF_{Cl} can be represented in the previously shown Equation 1.7 for lower amounts of Cl in the ESP ash.

$$2NaCl_{(c)} + SO_{2(g)} + \frac{1}{2}O_{2(g)} + H_2O_{(g)} \rightarrow Na_2SO_{4(c)} + 2HCl_{(g)}$$

(Rxn 1.14)

$$EF_{Cl} = \left(\frac{[\boldsymbol{Cl}]}{[Na]+[K]}\right)_{ash} \Big/ \left(\frac{[Cl]}{[Na]+[K]}\right)_{liq}$$ **(Eq 1.7)**

2.2 Liquor Cycle Concentration

As the effects that K and Cl concentrations in the liquor cycle have on process operations were becoming more understood, a need for processes to operate at higher degrees of closure (i.e., less waste streams) increased. Consequently, strategies were developed to control and deal with these larger K and Cl concentrations resulting in the liquor cycle, which can be employed by mills. Pfromm (1999) outlines some of the measures used to control high levels of Cl in the liquor cycle: increasing the amount of ESP ash purged and using lower Cl grades of caustic.

2.2.1 ESP Ash Purging

The rationale for increasing the amount of ESP ash being purged is a result of the ESP ash being highly concentrated in Cl (and K) relative to other purge points in the liquor cycle. As a result, large amounts of K and Cl can be removed from the liquor cycle by increasing the amount of purged ESP ash. The consequence of this additional purging is an increased operating cost associated with the additional make-up chemicals needed (such as caustic and saltcake) to replace the Na and S also lost with the purged ash (Pfromm, 1999).

The impact of ash purging was reported by Tran & Earl (2004) and Saturnino (2012). In the work by Tran & Earl (2004), operating data from a kraft mill was used to create a simple model of the recovery cycle. One of the results from this model suggested that a decrease in the Cl concentration of ESP ash from 3.0 wt% to 2.3 wt% and K concentration from 7.5 wt% to 6.5 wt% could be possible by increasing the amount of purged ESP ash. Similarly, in the work by Saturnino (2012) which developed a CADSIM model of a kraft mill, the effect of purging ESP ash was studied. It was found that a decrease in the molar ratio of Cl in the ESP ash from 4.2 % to 3.1% and molar

ratio of K from 2.1 % to 1.8 % was possible for the hypothetical mill considered by increasing the amount of purged ESP ash.

2.2.2 Caustic Grade

The rationale for using lower Cl grades of caustic, such as membrane grade, over more common and less expensive grades, such as diaphragm grade, is a result of large amounts of Cl entering the liquor cycle coming from wood, process water, and make-up chemicals like caustic. The use of these low Cl grades of caustic effectively removes one of the major contributors of Cl input to the liquor cycle, which ultimately lowers the Cl concentration in the liquor cycle (Pfromm, 1999).

The impact this switch can have on Cl concentrations in the liquor cycle was illustrated by Tran & Earl (2004). One of the results from this model, as previously mentioned, suggested that a decrease in the Cl concentration of ESP ash from 2.3 wt% to 1.7 wt% could be possible by switching from diaphragm grade to membrane grade caustic.

2.3 Literature Knowledge Gap

In literature, a few variables have been studied relating to recovery boiler operations that affect the K and Cl concentrations found in ESP ash. This work attempts to explain an unusual trend that is observed in the Cl concentration of ESP ash of an operating kraft recovery boiler using the knowledge currently available in literature. This was done to identify potential gaps in knowledge that may currently exist in literature pertaining to recovery boiler operations and the concentration of Cl in ESP ash.

2.4 Liquor Cycle Modelling

Modelling in the pulp and paper industry, as in many industries, is fundamental for understanding and improving operations. The models often rely on process simulators, such as CADSIM or WinGEMS, and typically focus on specific areas of the recovery cycle such as digestors, recovery boilers, etc. These simulations can provide general and in-depth understanding of the complex processes they model, but they often require specific and in-depth data to operate. While these models are effective at simulating their individual processes, it can be challenging to incorporate them at a larger scale, such as in models of the entire liquor cycle.

Attempts at modelling the entire liquor cycle have been done before by various authors including Lundström (2007), Saturnino (2012), and Andersson (2014). These attempts either require large amounts of specific and in-depth data or lack the ability to dynamically model the liquor cycle in a meaningful way.

A full mill model was developed for a Brazilian kraft mill in CADSIM by Saturnino (2012). This model utilized several developed modules across the 3 digesters, 5 evaporation plants, 3 recovery boilers, and 3 causticizing plants. Results from this simulation included the Na, S, K, and Cl concentrations in the liquor cycle and ESP ash with different ash treatment systems.

A simulation of NPEs, such as Cl and K, in the liquor cycle of a theoretical kraft mill was conducted by Lundström (2007). This model utilized a theoretical reference mill developed by STFI-Packforsk in WinGEMS. Results from this simulation included Na, S, Cl, and K concentrations in the liquor cycle and various outputs, including ESP ash, grits, dregs, etc. These results, however, were limited to steady-state operation.

A simulation of the Na/S mass balance of the liquor cycle of a Finnish kraft was conducted by Andersson (2014). This model utilized an existing WinGEMS model of the mill, which was updated for the current layout and production of the mill. Results from this simulation included the Na and S concentrations limited to the liquor cycle.

2.4.1 Simplified Mathematical Modelling

A mathematical model of a species in a simplified kraft liquor cycle was developed by Saturnino (2012). The purpose of this modelling was to explain results obtained from an in-depth full mill CADSIM simulation, as well as to find trends of the species in the liquor cycle based on operating parameters. This simplified model assumed that the flow rate of species into the liquor cycle was much less than the amounts flowing in the liquor cycle, and that the entire liquor cycle can subsequently be represented as a single CSTR. This CSTR model, as well as the results from this modelling, will be discussed further in later chapters.

3. Methodology

3.1 Analysis of ESP Ash

Electrostatic precipitator ash (ESP) samples were collected and analyzed for K and Cl content internally by the mill. Analyses of the ash samples were conducted with a Hach DR3900 spectrophotometer.

For the analysis of K in the ash, 0.1 g samples of ash were weighed and mixed with deionized water to form a 250 mL solution. A secondary dilution, with a dilution factor of 4, was performed on the solution. The K concentration of this resulting solution was determined using the Hach (2014) Method 8049: Potassium, Tetraphenylborate Method.

For the analysis of Cl in the ash, 0.1 g samples of ash were weighed and mixed with deionized water to form a 250 mL solution. The Cl concentration of this solution was determined using the Hach (2018) Method 8113: Chlorine, Mercuric Thiocyanate Method.

The mill collects samples of the ESP ash semi-regularly once or twice a week for K analysis and regularly up to 3 times a week for Cl analysis. The trend of the K content in the ash can be seen in Figure 3.1. There are no noticeable periodic trends observed in this potassium content, and the concentration is currently around 6 wt%. The trend of the Cl content in the ash, Figure 3.2, appears cyclical with Cl contents between 0.5 - 1.4 wt%. The period of this observed trend, as measured by the distance between maximums, was determined to be around one year.

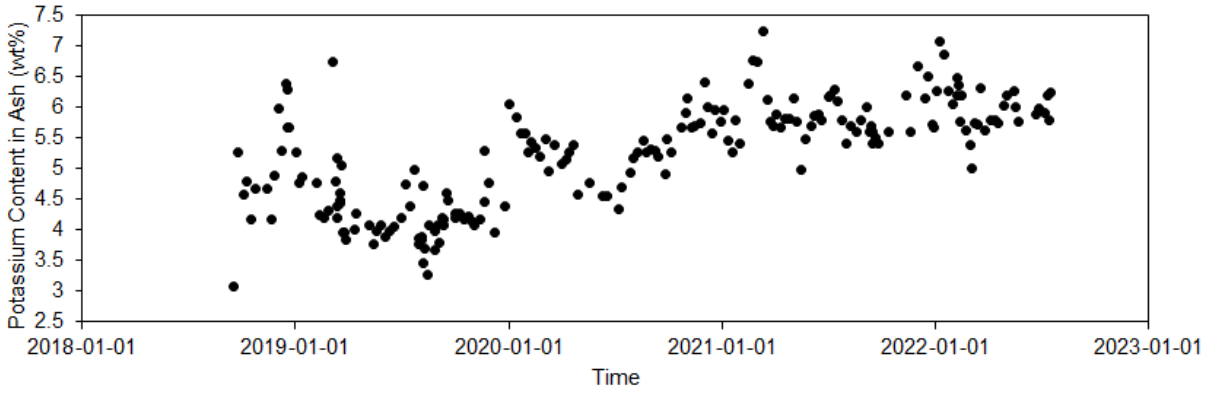

Figure 3.1: Trend observed in the K content of ash.

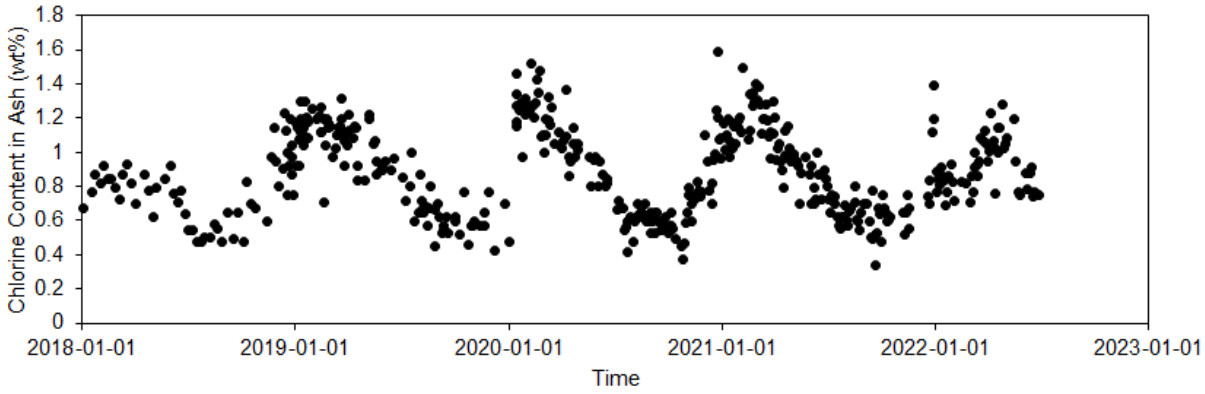

Figure 3.2: Trend observed in the Cl content of ash.

Due to the cyclical nature which was observed in the Figure 3.2 trend, a comparative analysis was conducted on the observed trend. For this comparative analysis, the trend was separated into individual cycles, as shown in Figure 3.3, which were determined by the observed maximums of the data. These resulting individual cycles will be compared to identify any potential similarities in this observed cyclical trend.

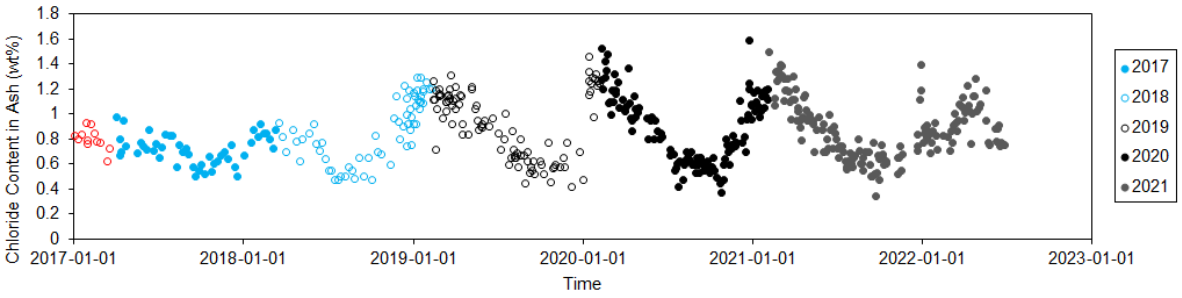

Figure 3.3: Individual cycles of the observed Cl trend of ESP ash.

3.2 Analysis of Process Variables

Due to the high Cl content observed at the beginning of the 2019 year shown in Figure 3.2, a campaign began in which numerous samples of ESP ash and black liquor were collected and sent for external analysis. These samples were collected to better understand the concentrations of the K and Cl in the liquor cycle. This sampling period, which lasted nearly 390 days, consisted of over 80 ash samples and over 60 liquor samples being collected and sent for analysis by an external lab. From this analysis, the concentrations of Na, S, K, and Cl were determined for the ESP ash and the black liquor during this time.

3.2.1 Sample Preparation

Liquor samples were initially prepared by diluting the liquor samples with distilled water to a concentration of 20 – 30 % and storing them under refrigeration. This was done so that they could be handled as a fluid in accordance with the TAPPI (1999) T650 om-99 method of determining the solids content of black liquor. Additional preparation of the liquor samples for analysis followed the TAPPI (2000) T699 om-00 method of analysis of pulping liquors by suppressed ion chromatography (IC).

Ash samples were prepared for analysis by adding 1 g of the ash sample into a tared container and approximately 50 mL of de-ionized water to completely dissolve the ash.

3.2.2 Sample Analysis

The Cl concentration of the samples was determined by IC in accordance with the TAPPI (2000) T699 om-00 method of analysis of pulping liquors by suppressed ion chromatography. The IC system was set up following the manufacturer's instructions and working standards were injected to calculate the regression of the linear range. The prepared solutions were diluted as needed to bring the Cl concentration of the samples into this linear range.

The concentrations of the remaining species (Na, S, and K) were determined by mass spectroscopy inductively coupled plasma (MS-ICP). The ICP system was set up following the manufacturer's instructions and working standards were injected to calculate the regressions of the linear ranges. The prepared solutions were diluted as needed to bring these concentrations into their respective linear range. For each analysis, a 15 mL aliquot of the sample was filtered through a 0.22 μm membrane filter before injection into the ICP system.

3.2.3 Sample Enrichment Factors

Since the Na concentrations of the ESP ash and black liquor samples were determined during the sampling period, the trends of the K and Cl molar ratios, as defined previously in Equation 1.5, could be determined for the black liquor and ESP ash. These trends can be seen in Figure 3.4 for K and Figure 3.5 for Cl.

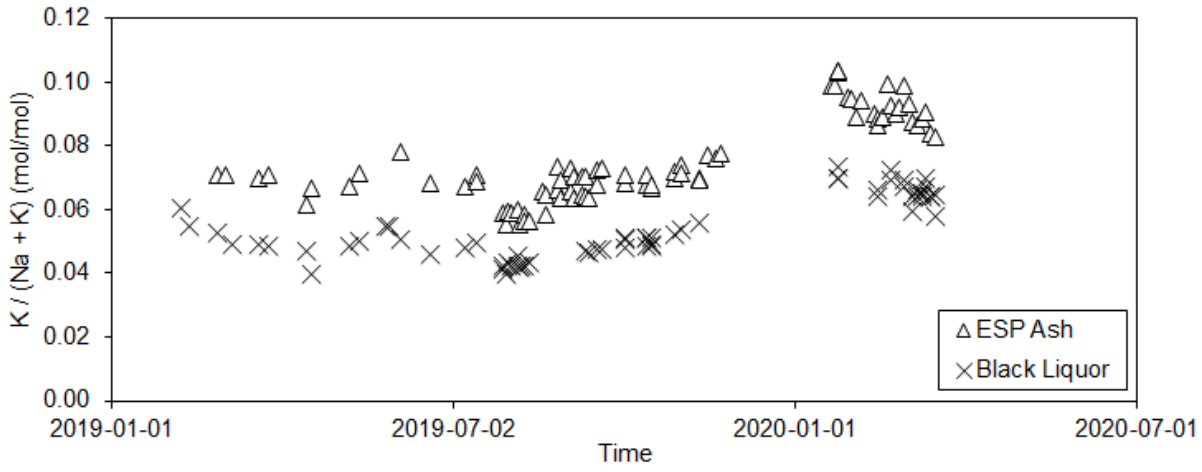

Figure 3.4: K molar ratios of ESP ash and black liquor during sampling period.

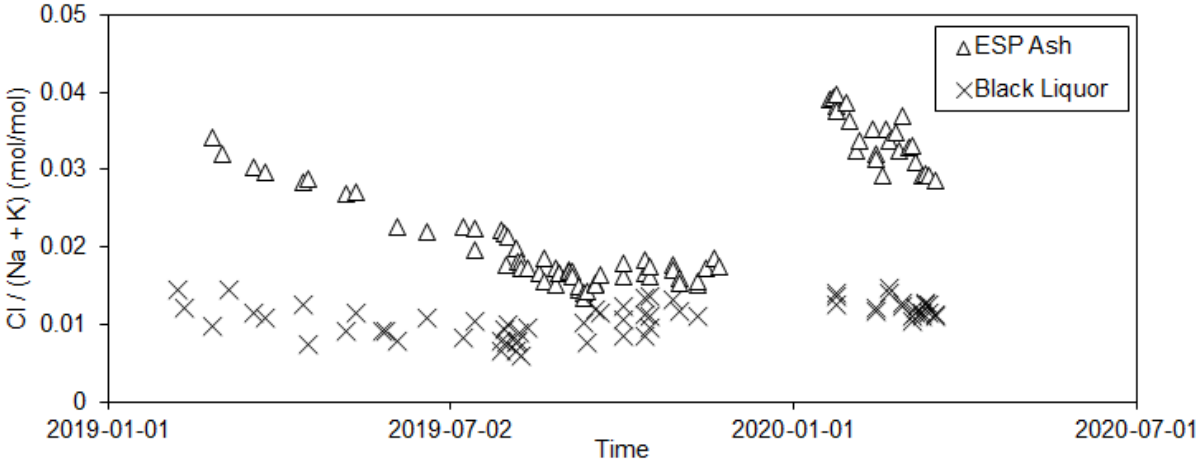

Figure 3.5: Cl molar ratios of ESP ash and black liquor during sampling period.

Figure 3.4 shows that the trend of the K molar ratio in the ESP ash is nearly identical in shape to the trend for the black liquor. However, Figure 3.5 reveals that the similarity in shapes are not as evident for the Cl molar ratios as they were for the K molar ratios. The ratio between the trend of the ESP ash and the black liquor is the previously discussed enrichment factor (EF), Equations 1.6 and 1.7.

For days in which both black liquor and ESP ash samples were collected, the resulting EFs were determined during the sampling period, Figure 3.6. The nearly identical trends, which were observed for the K in Figure 3.4, are represented as a nearly constant EF_K of 1.4. Nevertheless, the EF_{Cl} is not constant and varied significantly between 3.9 and 1.2 during this time.

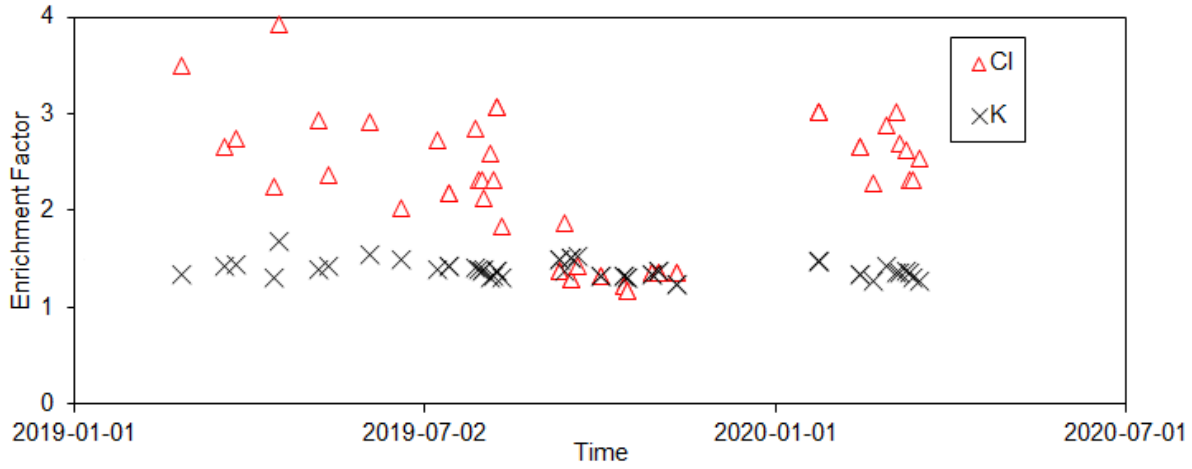

Figure 3.6: Resulting enrichment factors of K and Cl in ESP ash during sampling period.

3.2.4 Process Variables Analyzed

Since changes in enrichment factors are a direct result of changes in recovery boiler operation, an analysis was conducted for operating variables known to have an effect on enrichment factors. The following variables were considered:

- Lower furnace temperature
- Amount of combustion air
- SO_2 concentration in the flue gas
- Solids content of the liquor

Based on the simple trend which was observed in the Cl content of the ESP ash, which will be discussed later, an additional analysis was conducted for operating variables used to control Cl concentrations in the liquor cycle. This analysis included the following variables:

- Purging of ESP ash
- Grade of caustic

Data for the temperature of the lower furnace is currently not collected by the mill. Nevertheless, potential changes in lower furnace temperature were evaluated based on process variables which could affect the lower furnace temperature and are collected by the mill. This was limited to the temperatures of the following:

- Temperature of the combustion air
- Temperature of the fired black liquor
- Temperature of the furnace wall cooling tubes
- Temperature of the flue gas leaving the superheater

3.3 Liquor Cycle Mass Analysis

A mass analysis of Na, S, K, and Cl was conducted on the liquor cycle, shown previously in Figure 1.1. Species mass flow rates were calculated from stream flow rates available from mill data and concentrations which were determined by analysis from an external lab, Equation 3.1. Data available from the mill was either a mass flow rate (kg/min) or volumetric flow rate (L/min), and the concentrations were determined either by mass (kg/kg) or by volume (kg/L). In Equation 3.1, *b* denotes the stream and *a* denotes the species in that stream.

$$\dot{m}_{a,b} = \dot{m}_b \times C_{a,b} \; or \; \dot{V}_b \times C_{a,b} \qquad \textbf{(Eq 3.1)}$$

Assumptions which are based on best mill estimates can be seen in Table 3.1 and the additional assumptions used during the mass analysis are:

- The saltcake produced from the R10 process is pure Na_2SO_4
- The saltcake produced from the R11 process is pure Na_2SO_4 and a stoichiometric ratio of ClO_2 to Na_2SO_4 is achieved.
- The concentration of K and Cl in produced saltcake is negligible, based on low K and Cl concentrations from samples collected.
- The caustic solution is 50 % NaOH by mass. All Na present is in the form NaOH and remaining species are present as ions.
- The concentrations of all remaining input streams are constant and are determined as the numerical averages from samples collected.
- Species loss from the concentration of black liquor is considered negligible (the condensate is considered to be pure water).
- The moisture content of ESP ash is negligible.

- Stack emissions are an ideal gas at atmospheric pressure and the temperature of the flue gas exiting the recovery boiler.
- The amount of Cl lost with the flue gas (in the form of HCl) is 1/3 the concentration of SO_2 in the flue gas, based on the general rule of thumb by Vakkilainen (2006).

Table 3.1: Assumptions based on mill estimates used during mass analysis.

Stream/ Process	Value	Units
R10 Process Mass Yield	1.1	kg Na_2SO_4/ kg ClO_2
R11 Process Mass Yield	1.29	kg $NaClO_3$/ kg ClO_2
Andritz Digester Yield	0.456	AD kg pulp/ OD kg wood chips
Caustic Density	12.5	lb_m/gal
Annual Dregs Production	9,869,000	OD kg
Annual Grits Production	3,876,000	OD kg

3.3.1 Duration of the Mass Analysis

The duration for the mass analysis of the liquor cycle was chosen to be equal to the duration of the sampling period discussed previously. This period was selected in order to utilize the available data collected during this period, while still being long enough to minimize the effects of changes in the liquor concentrations and inventory levels throughout the process. The duration of the mass analysis, therefore, was from the beginning of March 2019 until the end of March 2020.

3.4 CADSIM Model

As mentioned previously, CADSIM was the software used to simulate the liquor recovery cycle as it is commonly used in the pulp and paper industry, can easily simulate dynamic conditions, and has easy integration with other programs such as Microsoft Excel to import dynamic data and export results. In order to create a CADSIM model, the stream chemistry (properties such as species, reactions, etc.) must be defined. Then, a flowsheet of the liquor cycle must be created (similar to a block flow diagram), which represents the streams and fundamental unit operations, called blocks or modules. Finally, the streams and processes (as they appear in the flowsheet) must be defined in accordance to the CADSIM modules used.

3.4.1 Defining Stream Chemistry

Water was the base species modelled, and additional user-defined species were created with the properties of water. The additional species include Na and S, since they are the main species of the liquor cycle; K and Cl, since they are the main NPEs to be modelled; and a miscellaneous species. This miscellaneous species is to represent the remaining species that make up the dissolved solids within the liquor cycle, such as C, H, O, etc.

CADSIM also allows for additional stream properties to be calculated. The following user-defined properties were created:

- A dissolved solids flow rate was determined as the sum of the Na, S, K, Cl and miscellaneous flow rates.
- A dissolved solids content was determined as the quotient of the dissolved solids flow rate to the total flow rate.

- Na, S, K, and Cl species flow rates were divided by the dissolved solids flow rate to calculate their respective mass concentration in the dissolved solids.
- Na, S, K, and Cl species flow rates were divided by their respective molecular weights for correct molar flow rates.
- Molar ratios of K and Cl, as defined in Equation 1.5, were obtained using the molar flow rates.

3.4.2 Creation of the Model Flowsheet

With the species now defined in CADSIM, the model flowsheet was created. The process flow diagram previously shown in Figure 1.1 was utilized as the flowsheet for the CADSIM model. The unit operations of the liquor cycle act as component splitters which have no volume associated with them. Consequently, tank modules (shown as CSTRs in CADSIM) were added to represent the volumes associated with the liquor cycle. This included the digester, black liquor inventory, green liquor inventory, and white liquor inventory. Based on the results of the liquor cycle mass analysis which will be discussed later, additions to the flowsheet were needed at two locations in order to utilize available mill data: prior to the recovery boiler area and prior to the digester. The resulting flowsheet of the CADSIM model can be seen in Figure 3.7.

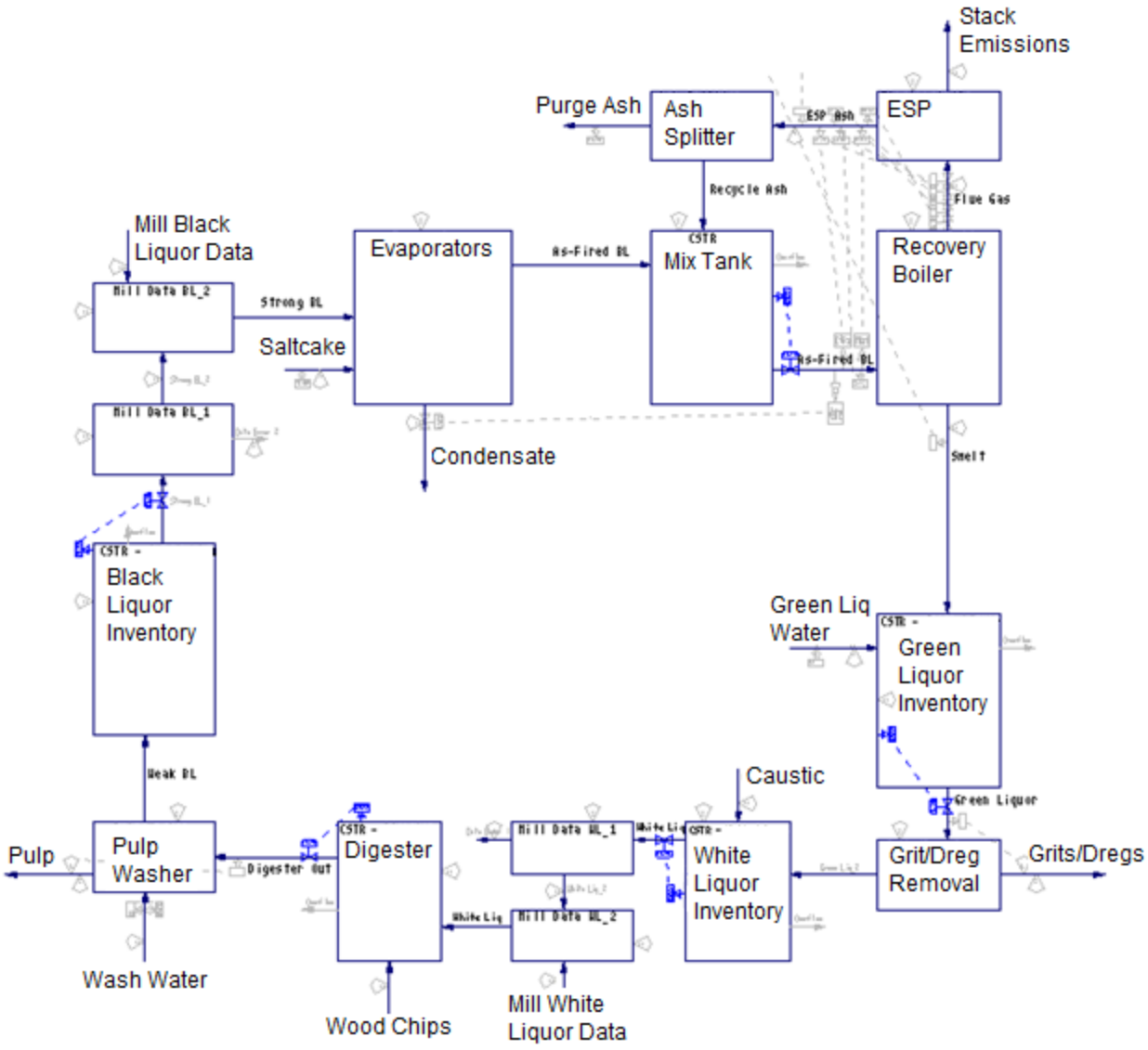

Figure 3.7: Flowsheet used in the CADSIM model simulation.

3.4.3 Defining Stream Properties

With the flowsheet completed for the CADSIM model, specification of all streams and modules were needed before simulation mode could be used. Since the model is a mass balance model focused on individual species, all temperatures throughout the model were set to CADSIM

defaults. Because of this, thermodynamic properties, such as density, were also constant. Since the species were created with the properties of water, the volumes of all tanks were scaled up based on their measured specific gravities to ensure that the residence times of the tanks matched those of the vessels they were modelling. The volumes of the liquor inventories were determined from the mill data averages over the duration of the mass balance, and the densities were obtained from mill data. All volumes in the model were kept constant using CADSIM controllers, shown as the control valves in Figure 3.7, and they were tuned using the CADSIM default tuning process. This was done to limit any errors associated with the controllers in the CADSIM software.

Based on the results from the mass balance which will be discussed later, the focus of the model was limited to the K and Cl species, and wood was the only input of K that was considered. Also, mill data was used to approximate Na and S flow rates into the recovery boiler area. Consequently, Na and S losses were only modelled in the recovery boiler area to ensure reliable concentrations needed for the modelling of K and Cl. Additionally, since the focus of the model was not on the Na and S balances, the flow rates of make-up chemicals (caustic and saltcake) were considered to be independent of the ESP ash purge flow rate.

3.4.3.1 Recovery Boiler Area

The recovery boiler area of the model can be seen in Figure 3.8, and the following assumption were made in the specification of streams in this area.

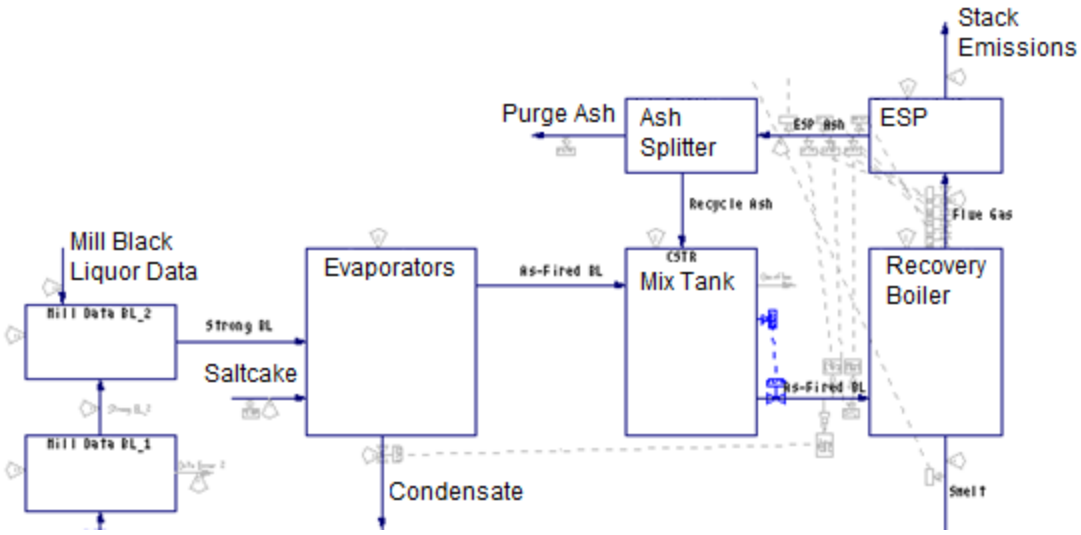

Figure 3.8: Flowsheet of the simulated recovery boiler area.

- The total and dissolved solid flow rates entering the recovery boiler area are manipulated to match mill data.
- The dissolved solids content of the black liquor entering the recovery boiler area (strong black liquor) and entering the recovery boiler (as-fired black liquor) are constant and determined from mill data.
- The saltcake is pure Na_2SO_4.
- The moisture content of saltcake is negligible.
- Only pure water is removed from the evaporators. The amount removed is manipulated to maintain the dissolved solids content of the as-fired liquor.
- The moisture content of ash is negligible.
- The flow rate of the recycled ash stream, known as the internal recycled dust (IRD), is constant. The flow rates used to define the IRD in Equation 3.2 are expressed in terms of dissolved solids.

- The IRD used is determined from the equation presented by Guimarães et al. (2014), Equation 3.3. The available total organic carbon (TOC) data was collected from liquor samples during the sampling period.
- The Na and S contents of the ash are constant and are determined from mill data.
- The K content of the ash is determined using a constant EF_K, as previously defined in Equation 1.6.
- The Cl content of the ash is determined using a constant EF_{Cl}, as previously defined in Equation 1.7.
- The amount of S lost in the stack is constant and determined from mill data. This includes the SO_2 and total reduced sulfur (TRS) such as H_2S.
- The amount of Cl lost in the stack (in the form of HCl) is 1/3 the concentration of SO_2 in the stack. This is based on the general rule of thumb by Vakkilainen (2006).
- No ash is lost with stack emissions.

$$IRD = \frac{\dot{M}_{IRD}}{\dot{M}_{As-fired\ BL}} \times 100\% \qquad \textbf{(Eq 3.2)}$$

$$IRD = \frac{TOC_{Strong\ BL} - TOC_{As-fired\ BL}}{TOC_{Strong\ BL}} \times 100\% \qquad \textbf{(Eq 3.3)}$$

3.4.3.2 Rest of the Liquor Cycle

The remainder of the liquor cycle in the CADSIM model can be seen in Figure 3.9. The following assumption were made in the specification of streams in this area.

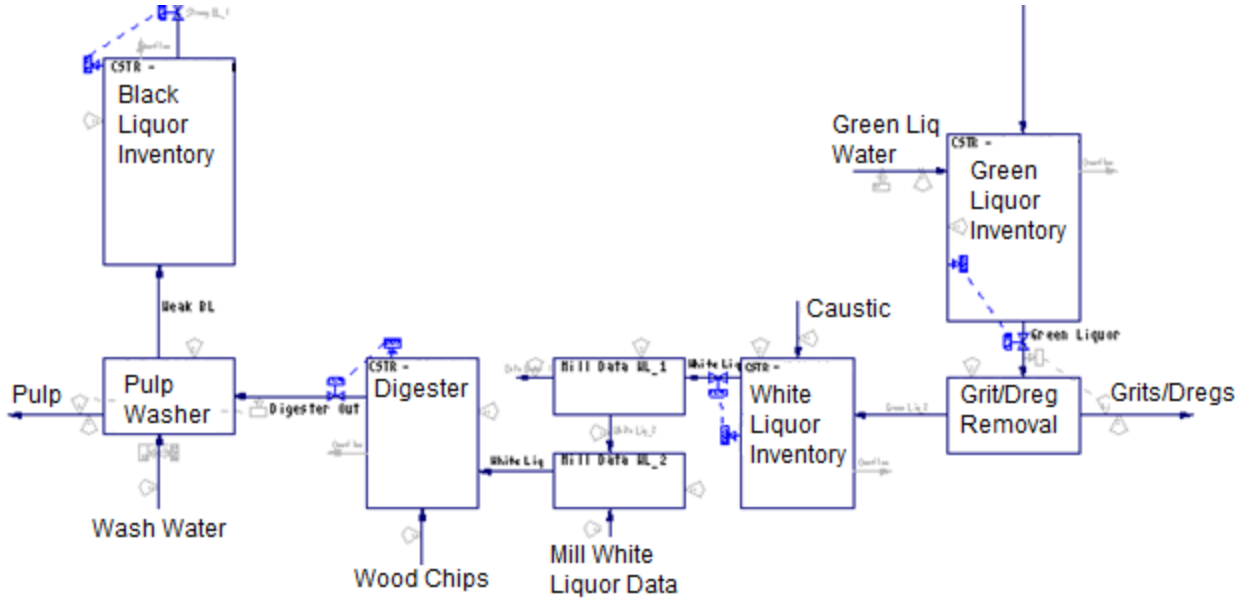

Figure 3.9: Flowsheet of the remaining simulated liquor cycle.

- The loss of Na and S with pulp, grits, and dregs are not considered.
- The Na and S flow rates in the white liquor entering the digester are manipulated to match mill data.
- The 14-day average of white liquor data is used to limit error in results from mill data variations.
- Loss of K and Cl to grits and dregs are a proportionality constant to their concentration in the liquor.

From samples of the washed pulp, it was found that the molar ratio of K, as defined in Equation 1.5, was nearly equal to its molar ratio in the resulting black liquor. However, the resulting Cl molar ratio in the pulp mat was found to be significantly greater than 1. This is most likely a result of the washing solution used: water containing a noticeable amount of Cl but not a significant amount of K or Na. This would suggest that the washed pulp mat contains some residual liquor

and some of the washing solution. Because of this, the CADSIM model used the following assumptions:

- The loss of K with pulp is proportional to its concentration in the liquor.
- The loss of Cl with pulp is both proportional to its concentration in the liquor and also proportional to the Cl in the washing water.

The proportionality constants used in the output of pulp were determined from available mill data.

From the limited samples of the grits and dregs, it was also found that the molar ratios of K were close to those of the liquor at that time. The amounts of grits and dregs produced by the mill are not measured and are based on unreliable mill estimates. Consequently, the following assumption were made:

- The loss of K and Cl to the grits and dregs are proportional to their concentration in the liquor.
- The losses associated with grits and dregs are lumped into a single outlet stream.

3.5.4 Simulation of the Liquor Cycle

Due to the unreliability of the grits and dregs flow rates, the proportionality constants associated with the grits and dregs were tuned during a calibration period. Calibration of these constants were obtained by modelling the K and Cl concentrations in the liquor cycle until the output best matched the available mill data. The model was then validated by testing its ability to replicate the K and Cl trends in ESP ash for an extended duration outside this calibration period.

Due to the availability of data in the liquor cycle, the calibration period was selected to be equal to the duration of the mass analysis: from the beginning of March 2019 until the end of March 2020. For validation, the model was run for an additional two years of data to test its capability of modelling the trends of K and Cl in the liquor cycle.

3.6 Simple CSTR Mathematical Model

It was mentioned earlier that the liquor cycle was previously represented and modelled as a CSTR by Saturnino (2012). This modelling was done to provide insight on the general behaviour of chemicals such as K and Cl within the liquor cycle.

Saturnino's model consisted of a single CSTR with a single inlet and a single outlet, shown in Figure 3.10, where *f* is an inlet flow rate (m^3/s), C_{in} is an inlet concentration (kg/m^3), *V* is the volume of the vessel (m^3), *Q(t)* is an amount of species within the vessel at a given time (kg), and *t* is time (s). The resulting equation from this modelling of the concentration within the tank over time can be seen in Equation 3.4.

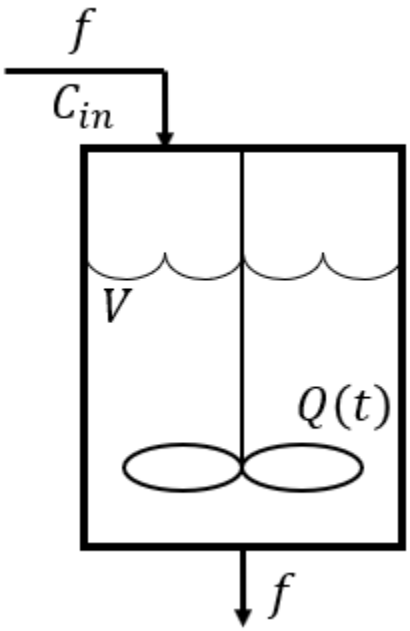

Figure 3.10: Schematic diagram of CSTR model presented by Saturnino (2012).

$$C = C_{in}\left(1 - e^{\left(-\frac{f}{V}t\right)}\right) + C_o e^{\left(-\frac{f}{V}t\right)} \qquad \textbf{(Eq 3.4)}$$

From this equation two conclusions were made: the concentration within the vessel given significant time (or once steady-state is reached) is dependant on and equal to C_{in} and the time to reach a steady-state value is dependant on the ratio f/V. While these conclusions are useful, they are unable to provide insight on notable trends obtained in this work which will be discussed later.

The significance in the purging of ESP ash, fundamentally, is to remove NPEs, such as Cl and K, from the liquor cycle. Other sources of Cl and K loss from the liquor cycle include the pulp produced, other purge streams such as grits and dregs, and liquor spills. However, the amount of ash purged is often manipulated and controlled to limit the loss of valuable cooking chemicals, such as Na and S, while still maintaining acceptable levels of K and Cl within the liquor cycle. Moreover, ash is significant because it is often more concentrated with K and Cl than the liquor cycle; this is evident by the previously shown enrichment factors being greater than 1. This means that ash can be purged to remove more K and Cl within the liquor cycle than other losses (pulp, spills, etc.) while losing less Na and S.

As a result, the model presented by Saturnino (2012) and shown previously in Figure 3.10, was expanded upon in this work to include a second outlet which is concentrated and partially purged, with the remaining solution being recycled to the vessel, Figure 3.11. The additional and renamed streams *a, b, g, h,* and *j* (in which *a* represents the concentrated ash stream and b represents other loses in the liquor cycle such as with liquor spills, pulp, etc.) are flow rates (m^3/s); C_a, C_b, C_g, C_h, and C_j are concentrations (kg/m^3) of their respective streams.

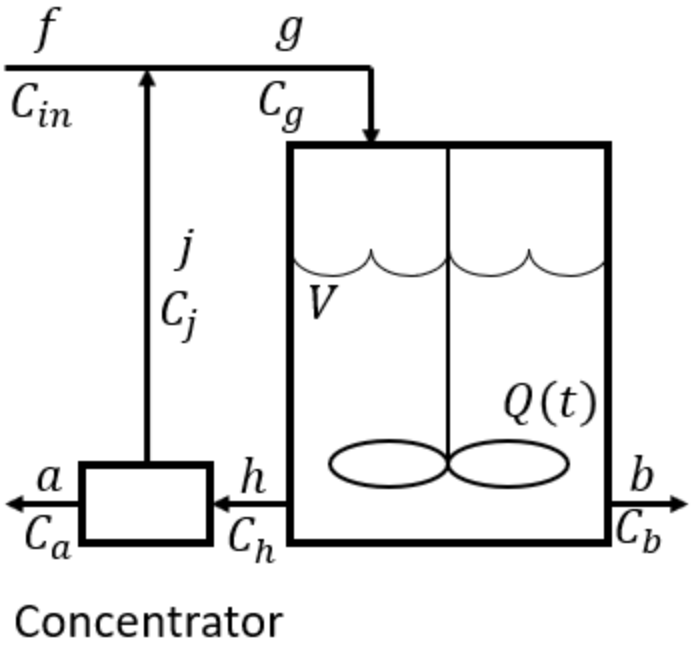

Figure 3.11: Schematic diagram of CSTR model in this work.

4. Results

4.1 Analysis of ESP Ash

Due to the similarities of the trends observed for the 2019, 2020, and 2021 cycles that were shown previously in Figure 3.3, they were directly compared first, Figure 4.1. Looking at Figure 4.1, all of the cycles behave similarly for the first 250 days while the concentration is decreasing. After this point, the trends for the 2019 and 2020 cycles follow a similar as the Cl concentration increases until the end of the approximately 360-day cycle. For the 2021 trend, however, at a point around 300 days, the Cl concentration in the ESP remains relatively constant at ~ 0.8 wt% for approximately 90 days. After this 90-day duration, the cycle appears to resume in a similar way to that of the end of the 2019 and 2020 cycles. In order to test this, the 90-day duration where the Cl content of the ash was constant was removed. This subsequent trend was compared to the previous cycles, Figure 4.2. From Figure 4.2, it can be seen that when the unusual 90-day duration of constant Cl content is removed, the 2021 cycle matches the trend of the previous cycles.

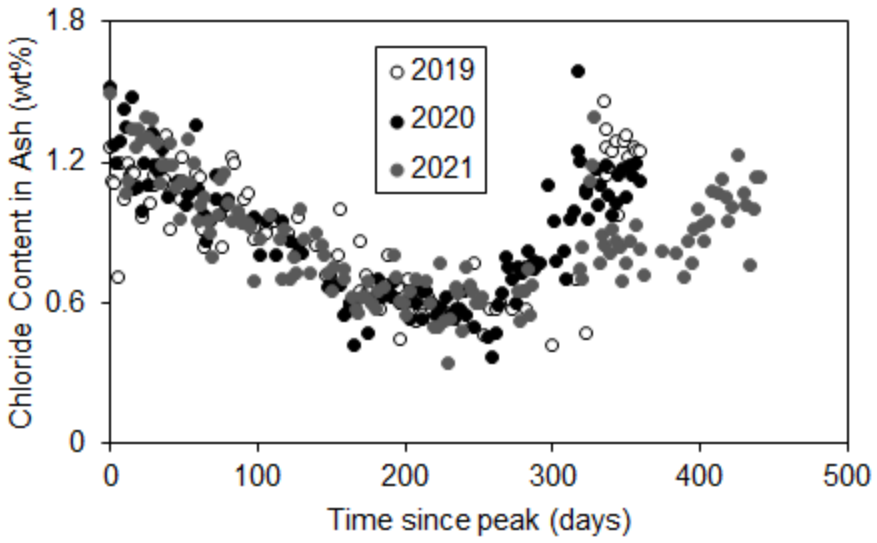

Figure 4.1: Direct comparison of 2019 to 2021 cycles.

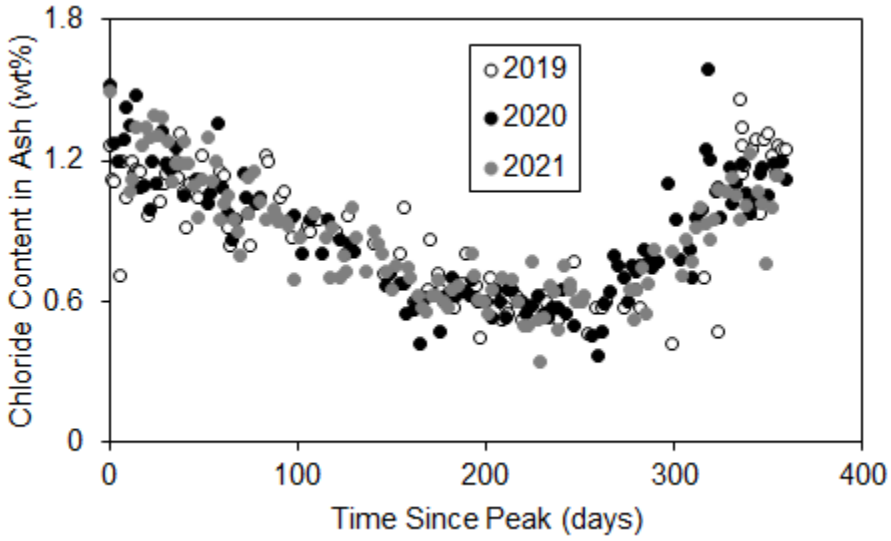

Figure 4.2: Direct comparison of resulting 2021 cycle to 2019 and 2020 cycles.

Since the trends of the 2017 and 2018 cycles do not have amplitudes comparable to that of the more recent years, the amplitudes of these cycles were normalized by setting their maximum to a value of 1 and their minimum to a value of 0, Figure 4.3. These cycles behave similarly over their slightly shorter period of approximately 340 days. This includes the duration when the Cl content

is increasing, despite the difference in the amounts they increased in the previously shown Figure 3.3.

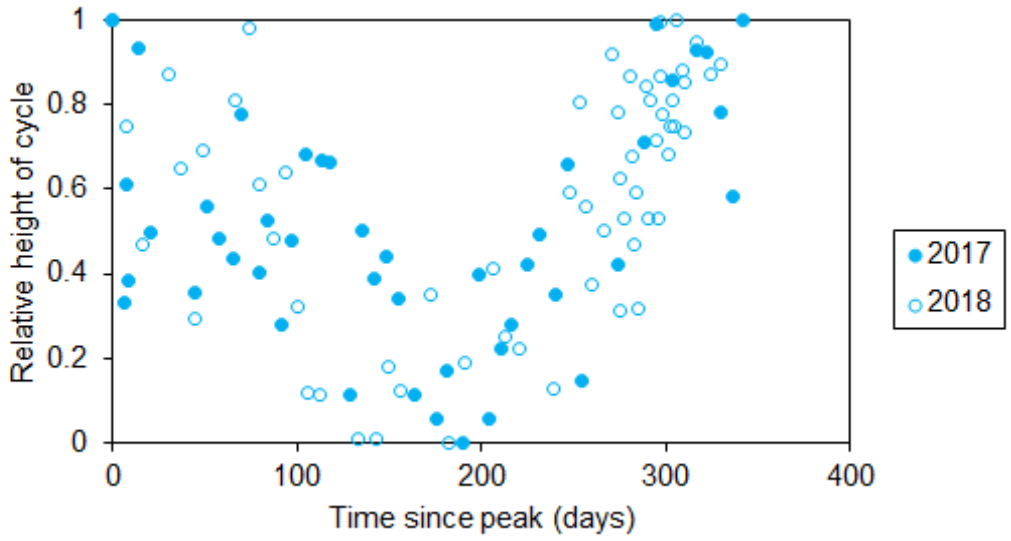

Figure 4.3: Direct comparison of 2017 and 2018 normalized cycles.

The trends for 2019, 2020, and 2021 were similarly "normalized" so that they could be directly compared with the trends for 2017 and 2018, Figure 4.4. Despite the slightly shorter period of the 2017 and 2018 cycles, all of these cycles have a similar shape. This result indicates that over a period of the past five years, the cyclical trend of the Cl content of ESP ash behaved in a simple and predictable way. The exception to this was the unusual 90-day duration observed in the 2021 cycle which was excluded.

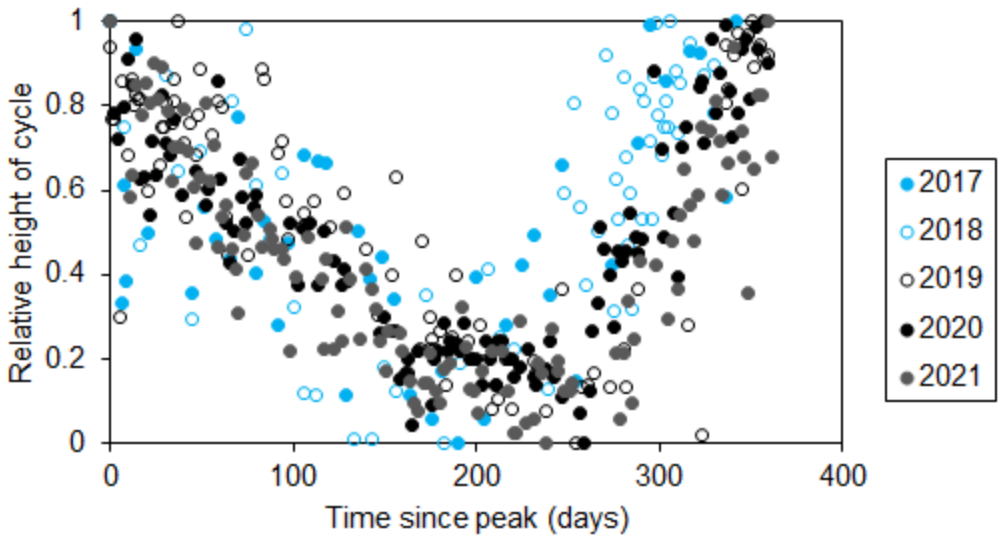

Figure 4.4: Direct comparison of 2017 to 2021 normalized cycles.

An investigation was conducted into this 90-day duration where the unusual trend was observed in the 2021 cycle. Results from this may provide potential insight into the cause of the observed trend. In order to investigate this period, mill data was analyzed during this period to identify any potential changes to operations at that time, and mill personnel were contacted for additional insight into the matter. One important finding was that this 90-day duration occurred directly after a major shutdown which lasted a significantly longer time than usual. However, no unusual maintenance was done to the recovery boiler during this time that differed from maintenance done during the past five years.

Through looking at available mill data and from the information provided by mill personnel, no significant results were found which would be able to explain the unusual trend observed in the otherwise predicable behaviour of the Cl content in the ESP ash observed over the past 5 years.

4.2 Analysis of Process Variables

4.2.1 Correction Factor of Internal Mill Data

During the sampling period, many samples of ash were collected and measured both internally by the mill and by the external lab. This allowed for the concentrations in the ash determined internally by the mill to be directly compared to those obtained from the external. This was done because they are measuring the same trend and, as such, should agree/be similar with one another. These comparisons can be seen in Figure 4.5 for K and Figure 4.6 for Cl.

For the comparison of K, the slope of the regressed line from this plot is quite close to 1 (0.9671), which would indicate that the internal measurement is replicating the measurement of the external lab. However, the low coefficient of determination (0.6545) indicates the regression is a weak fit to this data. Since the slope of the regressed trend is close to 1 (meaning the measurements are similar) but the coefficient of determination is low (stipulating the correlation is weak), no correction factor was applied to the K data.

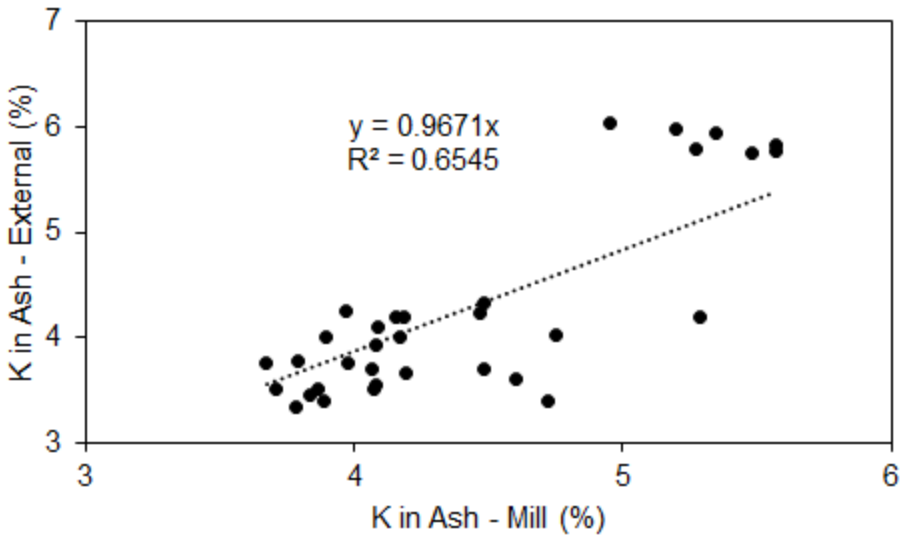

Figure 4.5: Comparison of concentration results for K in ESP ash.

Looking at Figure 4.6, the slope of the regressed line for the Cl data is quite different from 1 (1.5155), which would indicate that the internal mill measurements underrepresent the Cl content of the ash as measured by the external lab. Also, the high coefficient of determination indicates that the regression is a good fit to this data. This finding shows there is a significance in the underrepresentation in the internal measurement of Cl concentrations. As a result, a correction factor of 1.5155 was applied to the internally measured Cl data.

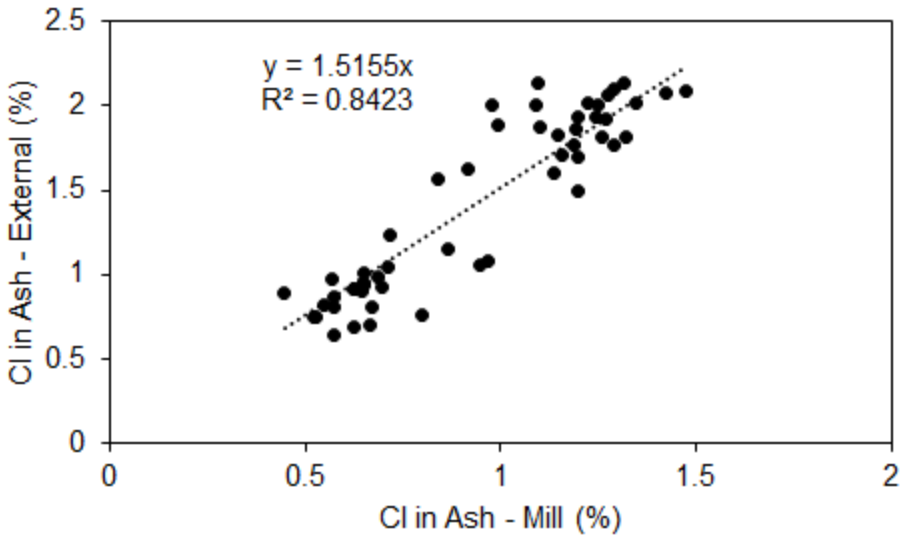

Figure 4.6: Comparison of concentration results for Cl in ESP ash.

4.2.2 Process Variables

All of the trends for the process variables that were evaluated can be found in Appendix A. Looking at the variables used to evaluate the lower furnace temperature (Figures A.1 to A.4), the temperature of the black liquor and the temperature of the wall cooling tubes of the recovery boiler showed no significant changes in their trends. Looking at the temperature of the combustion air, there was a significant step change in the temperature of the combustion air; however, the trend of the Cl content of the ash is not significantly different after this step change from the trend prior to this step change. Lastly, looking at the temperature of the flue gas after the superheater, there are some variations in the flue gas temperature during this period. Although, this trend is not similar in shape nor period to the trend of the Cl in the ESP ash. Furthermore, during the duration of the sampling period, in which the EF_{Cl} was known to change, there were no significant changes in the flue gas temperature. It is important to note that the temperature of the flue gas at this point, being

after the superheater, is also dependant on the heat transfer to the superheater sections. This means that deposit formation could also significantly impact this trend. Regardless, of these variables considered for evaluating the lower furnace temperature, there is no evidence at this time to suggest that changes in the lower furnace temperature can explain the changes observed in the trend of the EF_{Cl} nor the Cl content of the ESP ash.

Looking at the remaining trends of variables known to affect enrichment factors (Figures A.5 to A.7), the trends for the ratio of combustion air to liquor, the dissolved solids content of the black liquor, and the amount of SO_2 in the recovery boiler stack all show no significant changes during the sampling period. As a result, these factors cannot be the cause of the trends observed in the EF_{Cl} nor the trend observed in the Cl content of the ESP ash.

Looking at the variables known to control Cl content in the liquor, the trend of the purge flow rate of ash (Figure A.8) has significant variations in the ash purge flow rate over the duration observed. However, upon further analysis (Figure A.9), the trends of the purge strategy show no clear similarities when separated into corresponding periods from the previously discussed Figure 4.4. Consequently, there is no evidence to suggest that the purging strategy of ESP ash by the mill is able to explain the trend observed in the Cl content of the ESP ash.

Lastly, looking at the trend of the caustic grade used in the liquor cycle (Figure A.10), there was a switch in the grade of caustic used in the process during the sampling period. However, there is no change in the shape of the Cl trend after the switch of caustic grade from the shape of the trend prior to the change. Therefore, the change in the caustic grade cannot explain the trend observed in the Cl content of the ESP ash.

4.3 Liquor Cycle Mass Analysis

A table of available mill data and of stream compositions that were used for the mass analysis can be found in Appendix B, whereas the results from the mass analysis are shown in Table 4.1. Looking at Table 4.1, the discrepancy, which is the percent difference between the total outputs and the total inputs, is very large for Na and S (>50%). The input of S is largely observed to come from the saltcake (over 97% of all S input); in contrast, the input of Na has a majority from the saltcake (nearly 69%) but also a significant amount from the caustic (around 30%). This is expected, as the saltcake is the S make-up source while also containing a noticeable amount of Na, and the caustic is the remaining Na make-up source. Over half of all Na and S in the observed outputs come from the purged ESP ash, and a large amount of observed Na and S output also comes from the pulp. Although, a significant amount of Na and S is not accounted for in the mass analysis, represented by the large discrepancy value.

Table 4.1: Mass analysis of liquor cycle during sampling period.

Stream	Species Daily Average Flow Rate (kg/day)			
	Na	**S**	**Cl**	**K**
		Inputs		
Wood	68.0	138.5	98.2	1,205.9
Water	15.7	11.7	70.5	4.2
Saltcake	9,728	6,784	-	-
Caustic	4,209	3.6	52.6	1.9
Total Inputs	**14,021**	**6,938**	**221**	**1,212**
		Outputs		
Pulp	2,174	382.7	63.4	245.3
Flue Gas	-	102.7	25.5	-
Ash	3,389	1,605	142.9	474.8
Dregs	624.3	270.6	29.4	49.9
Grits	197.0	45.5	24.4	15.9
Total Outputs	**6,384**	**2,406**	**286**	**786**
Discrepancy (%)	**54.5**	**65.3**	**-22.5**	**35.2**

The mass analyses of K and Cl are observed to contain noticeably less discrepancies than those of Na and S. The majority of the K input into the liquor cycle (over 99%) is observed to enter with the wood; in contrast, the largest contributor to the Cl input is only a minority (around 44% from the wood) with the remaining amount observed to enter with the process water and the caustic. During the analysis duration, a switch from diaphragm grade to membrane grade caustic was made. As a result, the input of Cl from caustic may be significantly less after this period, as membrane caustic contains significantly less Cl than diaphragm grade caustic. The outputs of K and Cl also

largely come from the purged ESP ash. Also, the pulp is observed to contains a significant amount of the K and Cl output. The analysis of Cl was the only one in which the amount of outputs were larger than the inputs.

The lack of outputs found for the Na, S, and K may indicate that additional outputs have not been accounted for or that the quality of some output streams are insufficient. In contrast, the results from the Cl analysis may indicate that additional input sources of Cl input have not been accounted for. Further investigation of this will be discussed later.

4.3.1 Approximation of Na in the Liquor Cycle

Since the scope of the model is the K and Cl in the liquor cycle, an accurate amount of Na and S in the liquor cycle was needed for modelling. This was needed for the recovery boiler area in order to define concentrations, such as enrichment factors shown previously, Equations 1.6 and 1.7. The additional mill data needed for accurate modelling in the recovery boiler area was Na and S amounts in the liquor. The only area in the liquor cycle where such data may be available is in the monitoring of white liquor quality. These are determined for Na by the previously discussed TTA and for S by the previously discussed sulfidity of the white liquor.

If the amounts of Na and S circulating in the liquor cycle are much greater than the inputs to the liquor cycle, it would then be expected that the amounts of the Na and S in the liquor are similar at different locations in the liquor cycle. In order to test this, a comparison was of the Na flow rate in the liquor cycle was made between two points in the liquor cycle, Figure 4.7. The first point was in the white liquor, determined solely from available mill data. The other point was in the

black liquor, which was determined using mill flow rate data as well as using concentrations of the samples collected.

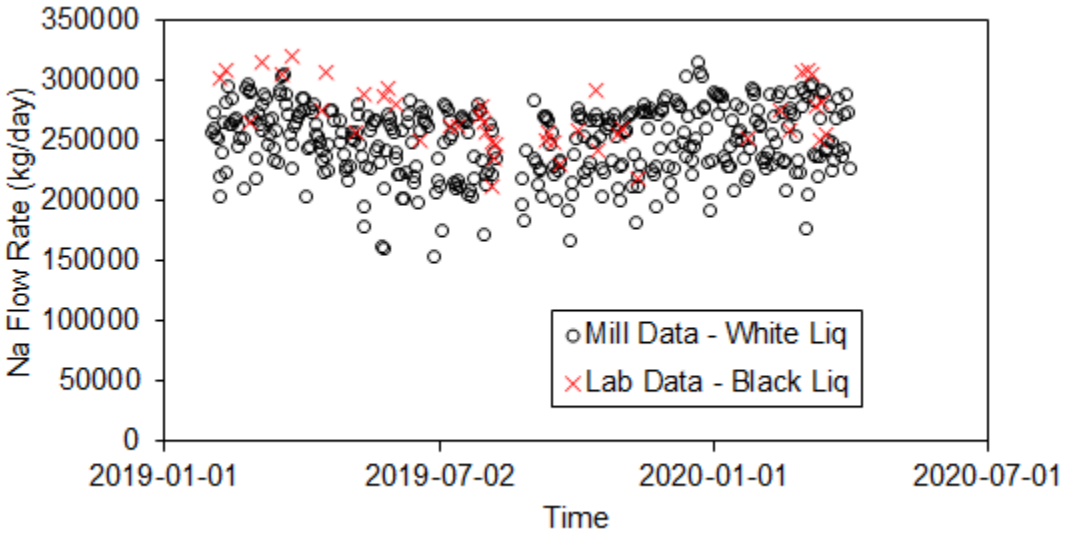

Figure 4.7: Comparison of Na flow in the liquor cycle.

The Na flow rate determined for the white liquor was found to be similar to the amount determined for the black liquor. As a result, mill data for the white liquor can be used to accurately represent the Na entering the recovery boiler area in the black liquor, which is needed for the modelling of K and Cl.

4.4 CADSIM Model

4.4.1 Calibration of the CADSIM Model

The calibration of the model consisted of tuning the amount of K and Cl loss in the grits and dregs to best fit the concentrations of black liquor. During this step, the concentrations of ESP ash were determined from available mill data and not from a constant EF_K or EF_{Cl}.

The loss of K to the grits and dregs was tuned to minimize the error between the resulting K concentration trend in the black liquor and the K concentration from the analysis of black liquor samples. The calibrated trend of the K in the liquor cycle during the calibration period, Figure 4.8, produced a good fit to the concentrations from the sample analyses.

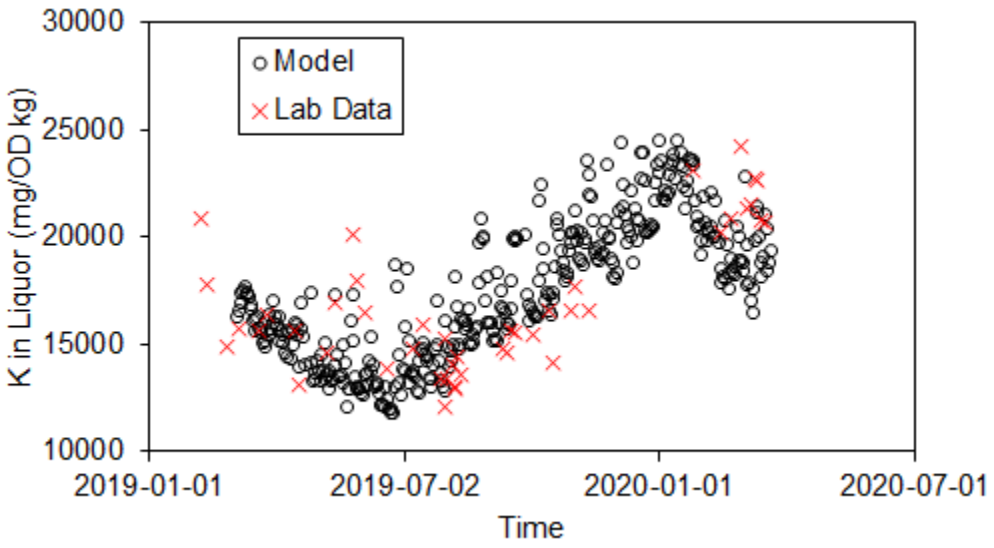

Figure 4.8: Resulting trend of black liquor K concentration during calibration period.

The loss of Cl to the grits and dregs was likewise tuned; however, as discussed previously, the observed amount of Cl into the liquor cycle was noticeably less than the observed outputs of Cl from the liquor cycle. Consequently, no amount of tuning to this loss of Cl was able to produce a

meaningfully good fit to the Cl concentrations measured. As a result, the proportionality constant for the loss of Cl to the grits and dregs was set to be equal to the value determined for that of K. Using this value, an amount of Cl input needed to reproduce the Cl concentrations obtained from the sampling period was determined using the available black liquor Cl concentration data, Figure 4.9.

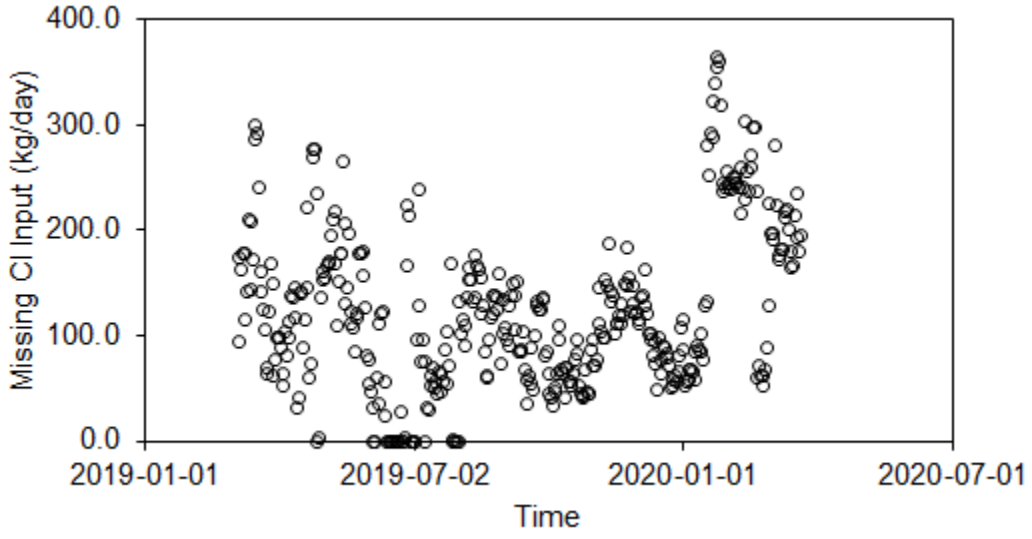

Figure 4.9: Missing Cl input determined during calibration period.

Looking at Figure 4.9, no clear trends are evident during this period. Looking at the middle of this duration when the amount of Cl missing is less than 200 kg/day, there appears to be a cyclical trend that is observed with a period of approximately 90 days. This trend, however, is less evident at the beginning and end of the calibration period. Also, larger amounts of Cl are observed to be missing during these times. This partial trend may be able to provide insight on the behaviour of a missing Cl input from the liquor cycle; however, at this time, no such inputs were found from available mill data nor from the insight of mill personnel. As a result, no conclusive results can be

meaningfully extrapolated outside of this calibration period and no additional Cl input was considered.

4.4.2 Validation of the CADSIM Model

4.4.2.1 Potassium

With the tuning of the model done, an extended simulation of the CADSIM model was done to test the performance of the tuned model to mill data outside the calibration period. Using the values obtained from the tuning, the CADSIM model was exposed to two additional years' worth of mill data.

Since data available for the liquor cycle is not available for the extended duration of the validation period, the resulting concentrations of the ash simulated from the CADSIM model were compared to the available mill data of the ash concentrations. Overall, the simulated K content in ash showed a good agreement with the trend of the mill data over both the calibration period (where the model now used a constant EF_K to simulate) and new data of the extended duration, Figure 4.10.

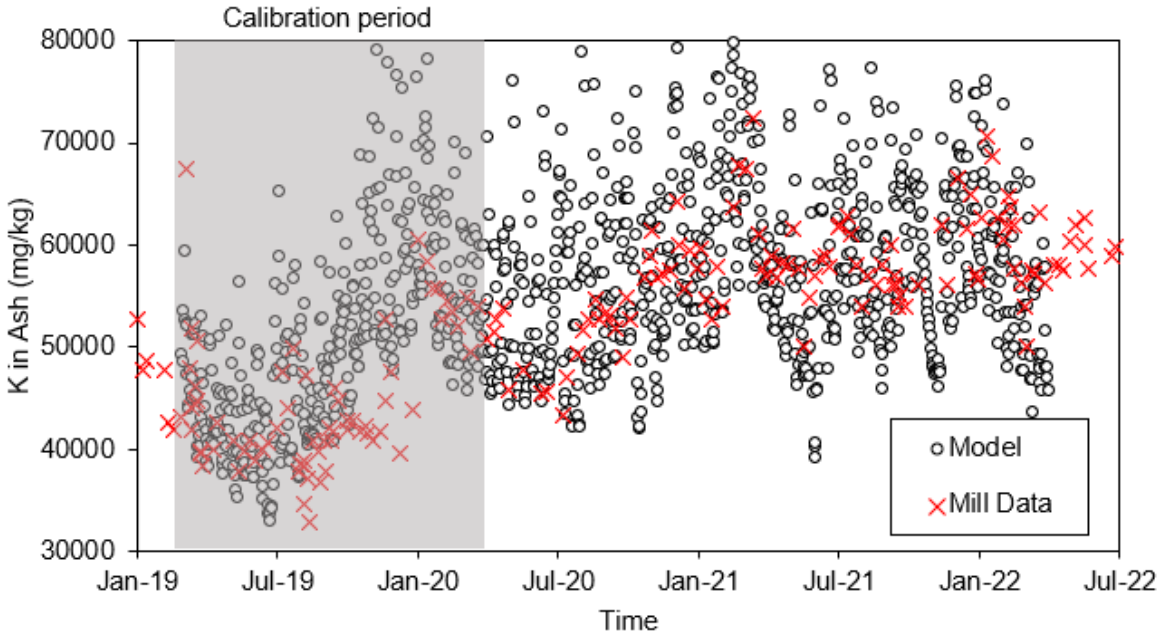

Figure 4.10: Resulting trend of K content of ash simulated from CADSIM model and mill data.

In order to test the significance of the proportionality constant determined from the calibration period, additional low and high concentrations of K in wood input, Table 4.2, were also tested. For these new inputs, the calibration process was repeated to find the resulting proportionality constants, and the validation process was then repeated. The resulting trends produced during these validation periods were nearly identical to the trend observed in Figure 4.10. The proportionality constants found at these inputs can be seen in Figure 4.11.

Table 4.2: Various K input concentrations used during K input sensitivity analysis.

Wood Chips K Content	Hardwood (mg/ OD kg)	Softwood (mg/ OD kg)
Low	850	300
Average	950	450
High	1100	550

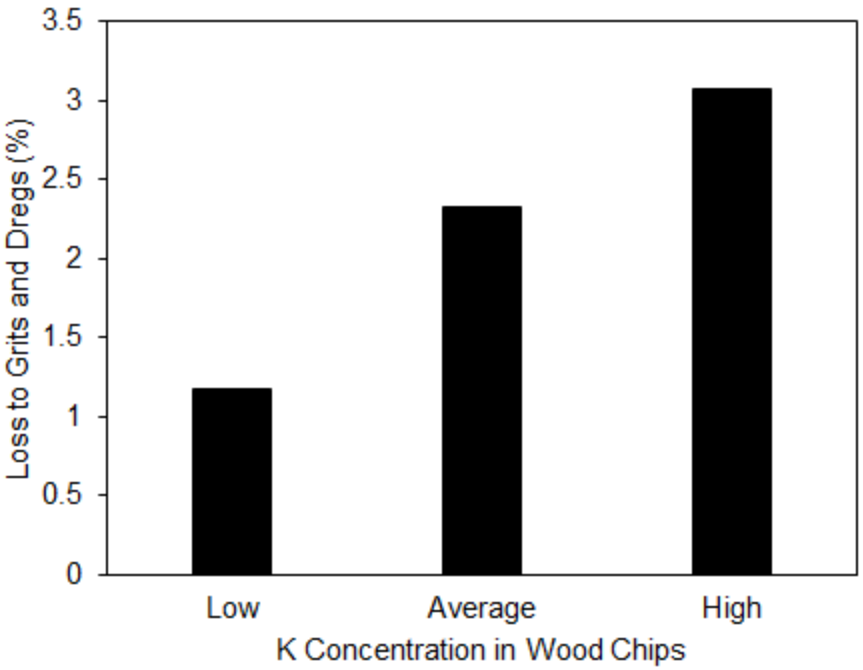

Figure 4.11: Proportionality constants determined at various K input.

Not only was a corresponding proportionality constant able to be determined during this sensitivity analysis, but the value found was also able to adequately replicate the observed trend during subsequent validation. This result indicates that the significance is not in the magnitude of the value determined, but rather for a given input of K, a corresponding value can be determined that is capable of replicating the trend observed in the mill data. As a result, the CADSIM model can be considered validated for predicting the trend of K in the liquor cycle and, subsequently, in the ESP ash.

4.4.2.2 Chlorine

An extended simulation of the Cl in the ash predicted from the CADSIM model was similarly compared to available mill data, Figure 4.12. The trend predicted for the Cl in the ash is unable to reproduce a trend similar to that observed in the mill data. This is partially expected because no additional missing Cl input that was considered, as discussed previously in the finding from Figure 4.9.

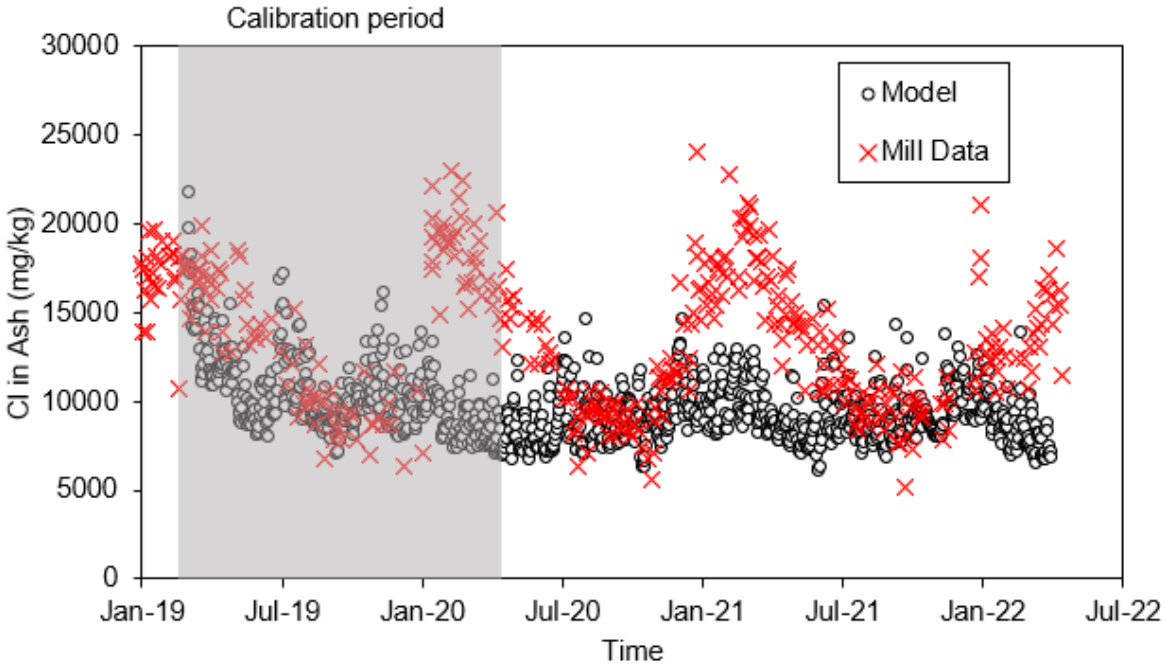

Figure 4.12: Resulting trend of Cl content of ash simulated from CADSIM model and mill data.

The CADSIM model's inability to reproduce the trend of Cl measured in mill data was also expected since the model assumes a constant EF_{Cl} in the recovery boiler. However, as seen previously in Figure 3.6, the EF_{Cl} values determined from the samples collected is not constant, but rather, it varied significantly between 1.2 and 3.9. As a result, multiple EF_{Cl} values were tested to determine how sensitive the results of the simulation are to the constant value selected. When

different EF_{Cl}s are tested, Figure 4.13, different regions of the trend observed in the mill data can be simulated by these values chosen.

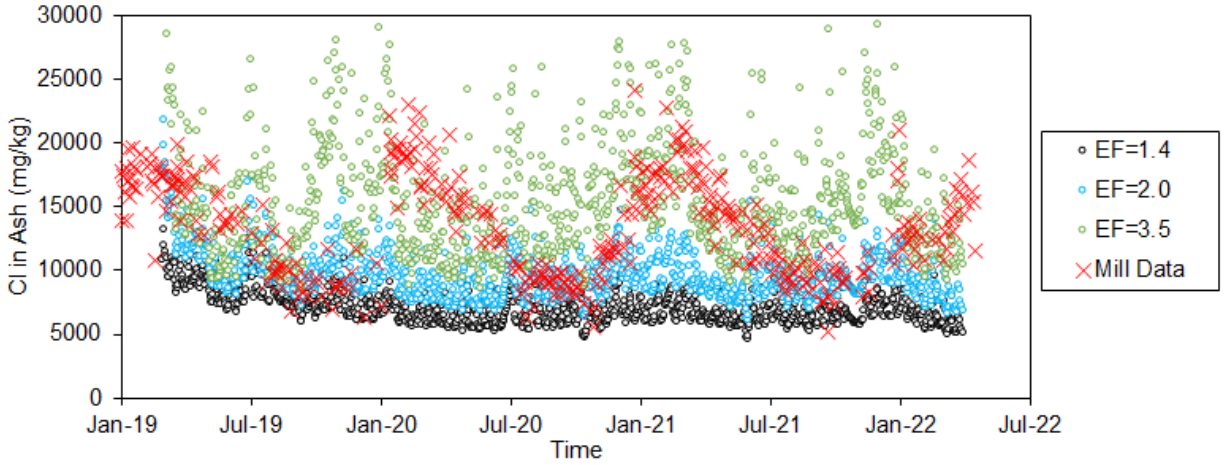

Figure 4.13: Resulting trends of Cl content of ash simulated with different EF_{Cl}.

Consequently, the trends from Figure 4.13 were separated into monthly sections to determine a EF_{Cl} value which best matched the trend observed in the mill data for each month. The result of this, Figure 4.14, is the trend of the resulting EF_{Cl} values which could hypothetically simulate the trend observed in the Cl concentration of ESP ash. This result indicates that an EF_{Cl} which varies over time is needed in order to reproduce the trend of the ESP ash Cl concentration observed from mill data. This finding of a varying EF_{Cl} is in agreement with the trend of EF_{Cl}s observed during the sampling period, shown previously in Figure 3.6. This would also suggest that a trend of varying EF_{Cl} values has continued past the sampling period and is still a current, unknown problem.

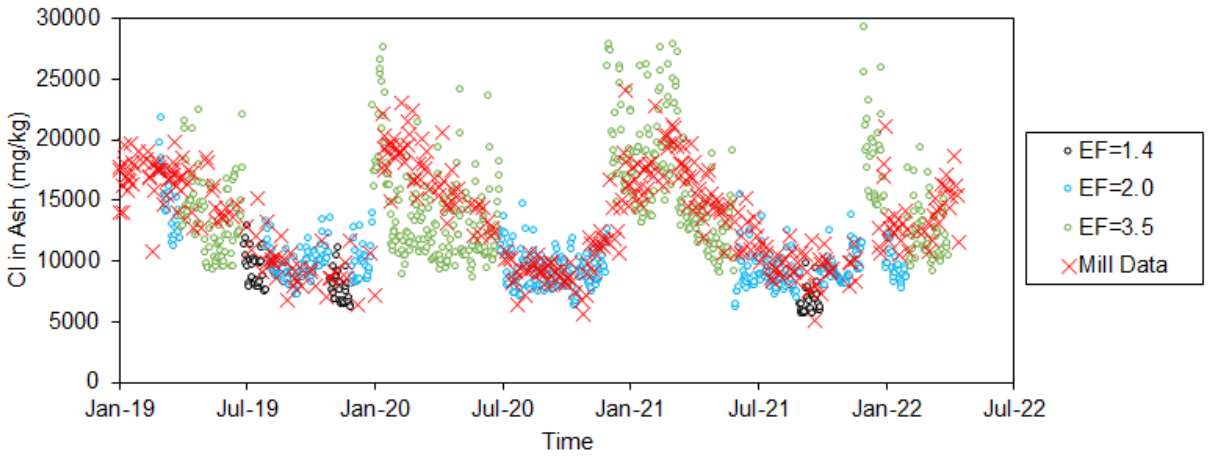

Figure 4.14: Resulting EF_{Cl}s required to hypothetically reproduce the ESP ash Cl content trend.

4.4.3 Additional Testing of the CADIM Model

The response of the CADSIM model was studied when a step change of a model variable is applied with constant input. The step change to be evaluated was chosen to be the ash purge flow rate. The constant inputs used were chosen to be the average of values during the validation period; however, the initial purge flow rate was selected to be 0 kg/day. During these tests, an EF_K=1.4 and an EF_{Cl}=2.0 were selected. The initial conditions were applied to the model and it was run until a constant value, or steady-state condition, was reached. At this time, t=0, the step change of the ash purge flow rate to 8000 kg/day was applied. Figure 4.15 is the response of both the K and Cl concentrations in the ash to that step change.

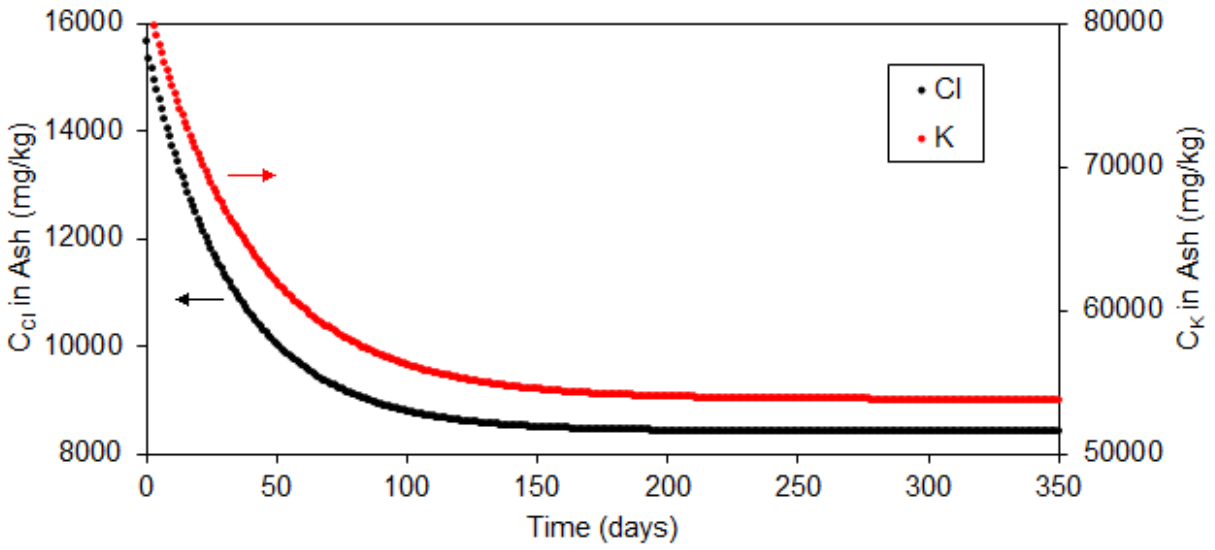

Figure 4.15: Ash concentration response to step change of ash purge flow rate.

For both of these responses, the rates of decrease in the ash concentrations appear to gradually decrease until reaching a steady value. Based on results from available literature, such as those presented by Saturnino (2012) as well as for reasons which will be shown in later sections, the response is expected to follow that of a first order response. The general equation of a first order response of a general term y, can be seen in Equation 4.1. The gain, K^0, is a constant which describes how much the system changes, and the time constant, τ, describes how quickly the system responds, or simply put, how fast the system reaches steady-state.

$$y = K^0\left(1 - e^{-\frac{1}{\tau}t}\right) \qquad \textbf{(Eq 4.1)}$$

If the response is expected to follow a first order response, as shown in Equation 4.1, then the rate of change in this response, with respect to time, would be the derivative of Equation 4.1 with respect to time.

$$\frac{dy}{dt} = K^0 e^{-\frac{1}{\tau}t} \qquad \textbf{(Eq 4.2)}$$

Equation 4.2 is in a form which can be easily regressed by software, such as Excel. As a result, the rates of change in the ash concentrations, as shown in Figure 4.15, were determined by the differences between subsequent points in the ash concentrations, Figure 4.16. For simplicity and clarity, only the absolute value of the rates of change are shown.

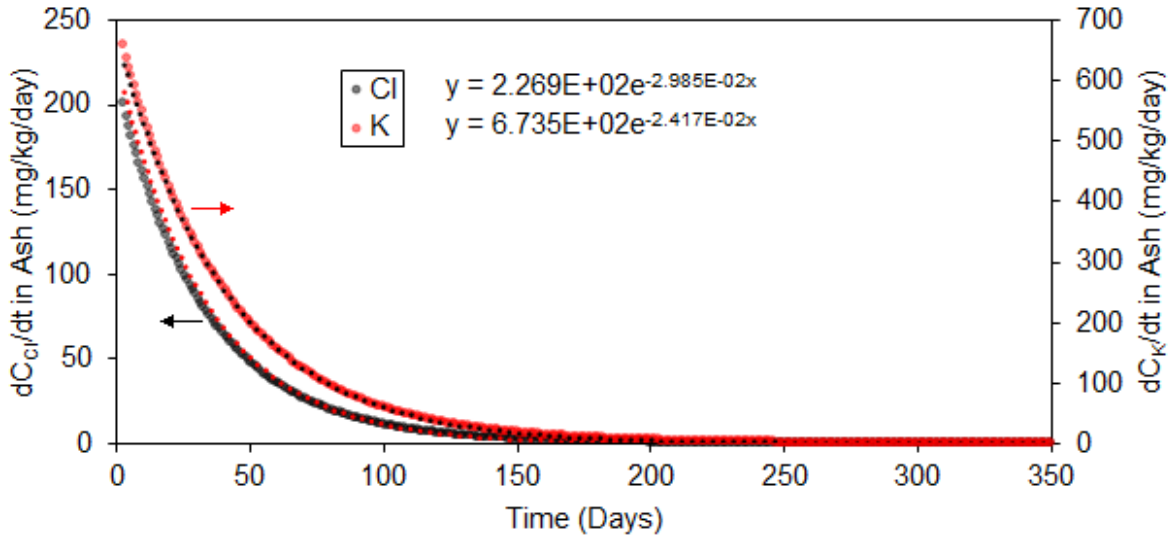

Figure 4.16: Rate of change in ash concentration response to step change of ash purge flow rate.

Looking at Figure 4.16, the trend of the K appears to approach 0 slower than the trend of the Cl. Also, the magnitude of the exponential constant, which allows for the determination of τ, determined by Excel for the K trend (-2.417×10^{-2}) is different from the constant determined for the Cl trend (-2.985×10^{-2}). This would suggest that the time required for the trends of K and Cl to reach steady-state values may not be equal. This trend from the CADSIM model clearly follows the response of a first order process, as the trend matches that predicted for one by Equation 4.2. Also, this shows that a method for determining the time constant, τ, is possible using Excel.

Using this method, time constants, τ, can now be determined at various ash purge flow rates, Figure 4.17. Looking at Figure 4.17, the time constants are nearly equal at a purge flow rate of 0 kg/day,

but as the purge flow rate increases, the time constants decrease. In contrast, the difference between the K and Cl time constants increases, and the K time constant is always larger than the Cl time constant.

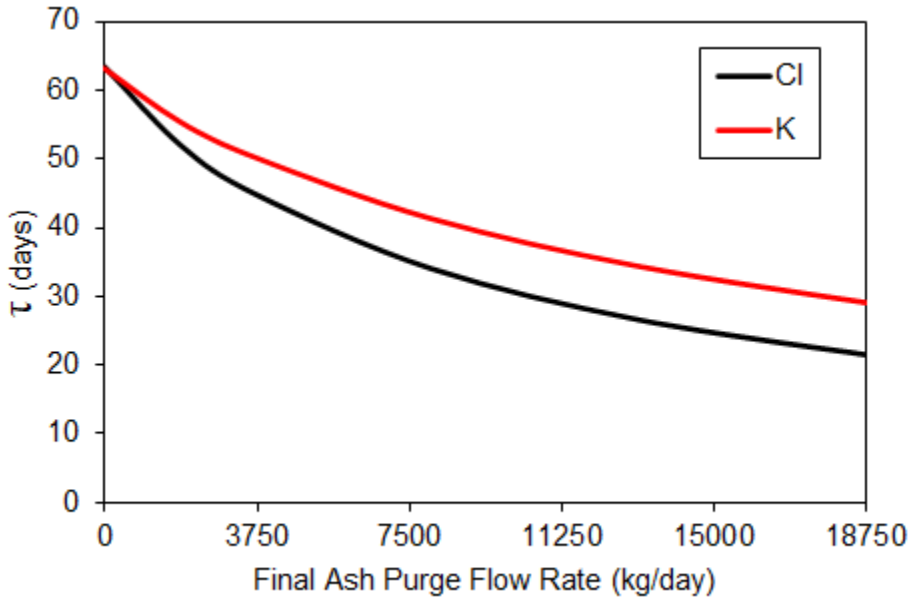

Figure 4.17: Time constants, τ, determined at various purge flow rates.

For reasons which will be discussed later, the inverse of this trend, 1/τ, was also found, Figure 4.18. Looking at Figure 4.18, these trends produced appear to be highly linear, which will, again, be discussed later.

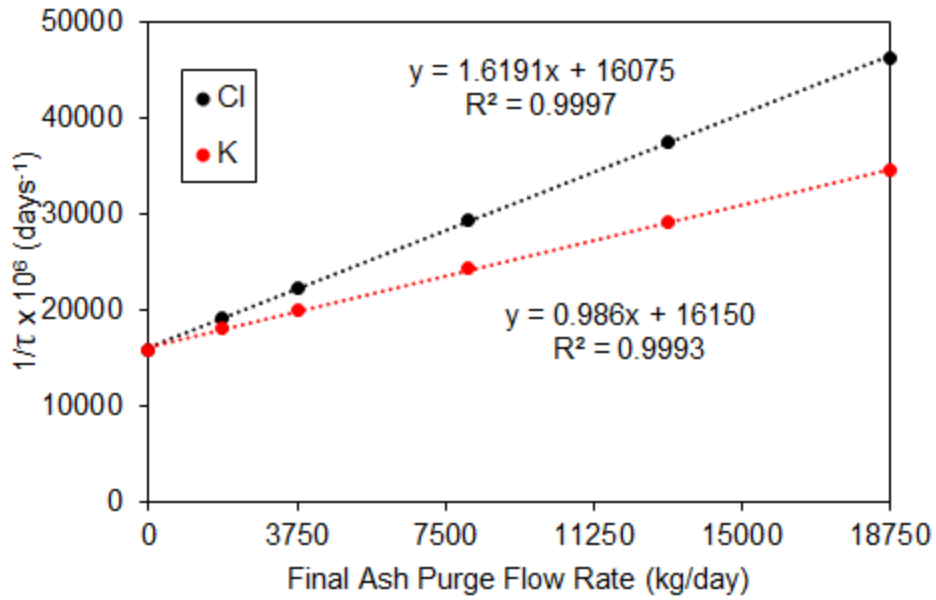

Figure 4.18: Inverse time constant, 1/τ, determined at various purge flow rates.

Since it was determined that the response of the ash concentration to a step change of the ash purge flow rate behaves similarly to a first order response, the well-known understanding of the first order response can be used to determine when steady-state is reached. It is well known that a first order response reaches 63.2% of its final value when t=τ. Other well-known values include, 95% of the final value being obtained at t=3τ and 99% of the final value being obtained at t=4.6τ. It was determined that an acceptable steady-state value is one which is at least 99% of its final value is reached. This means for determining the steady-state concentrations of the CADSIM model, at least 4.6τ time must be simulated. Also, since K always has a larger time constant, it will define when steady-state values are obtained. Lastly, since the time constant changes as the purge flow rate changes, the length of simulation will be dependant on the purge flow rate selected.

Using this definition of an acceptable steady-state concentration, the trend of the steady-state concentration of the ash can be determined at various purge flow rates, Figure 4.19. For both K

and Cl, the concentrations decrease as the purge flow rate increases. Surprisingly, the shape of these resulting trends obtained are similar to those obtained by Saturnino (2012) despite the differences in the purge flow rates shown. The purge flow rates selected in this work are based on limitations of the mill equipment; whereas, the purge flow rates shown in Saturnino's (2012) work are based on theoretical available ash produced.

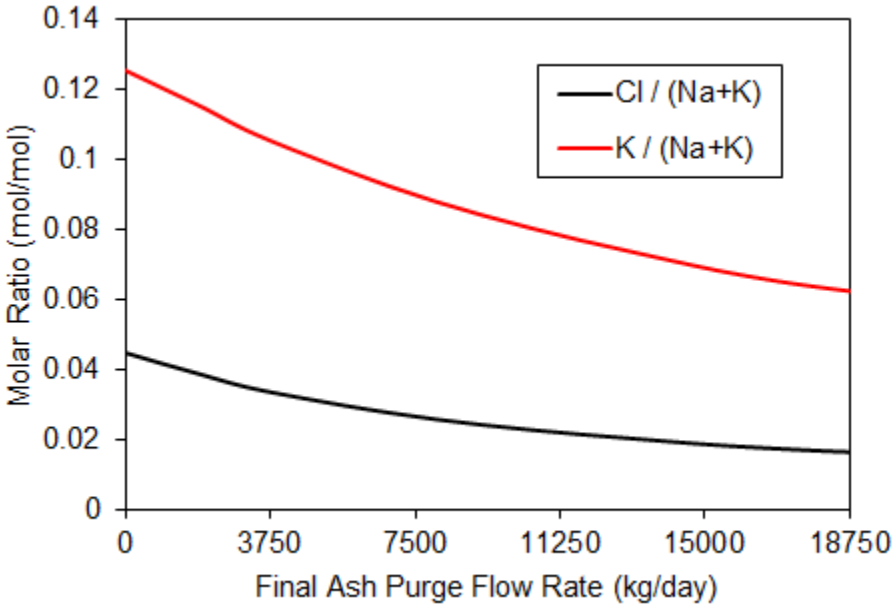

Figure 4.19: Steady-state concentration of ash at various ash purge flow rates.

For reasons which will, once again, be discussed later, the inverse of this trend was also found and can be seen in Figure 4.20. Looking at Figure 4.20, these trends are also linear. This linear trend, however, can explain why the trends found in Figure 4.19 were similar to trends found in previous works of literature: the inverse of a line would appear similar regardless of the domain (ash purge flow rates) selected.

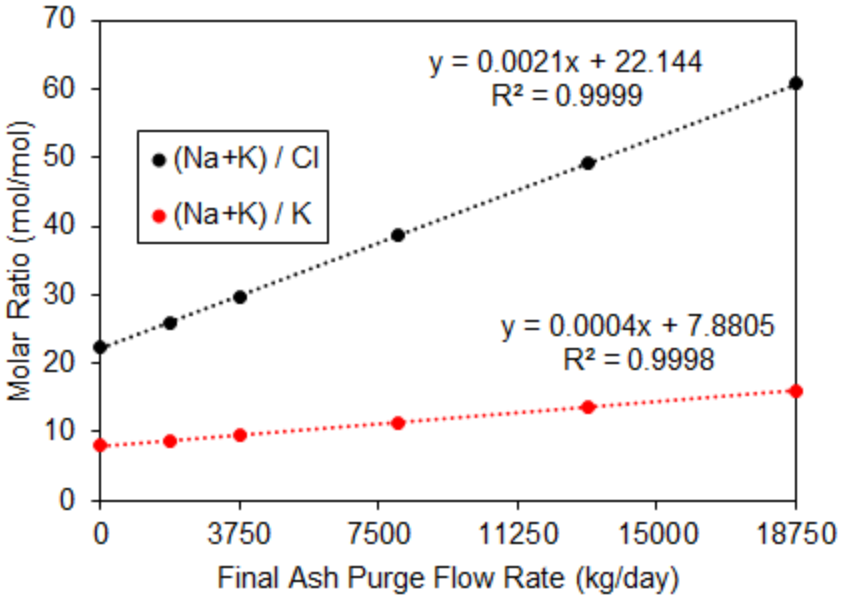

Figure 4.20: Inverse steady-state concentration of ash at various ash purge flow rates.

Lastly, the sensitivity of the model's results to the IRD selected was tested by evaluating the response of the model at different IRD values selected. The resulting trend of IRD on the inverse steady-state potassium concentrations can be seen in Figure 4.21. Looking at Figure 4.21, the IRD selected does have a large effect on the concentration found by the model. An increase to the IRD selected results in the linear trend previously found in Figure 4.20 being vertically translated downwards. While the results are not shown for Cl, a similar vertical translating trend was also observed.

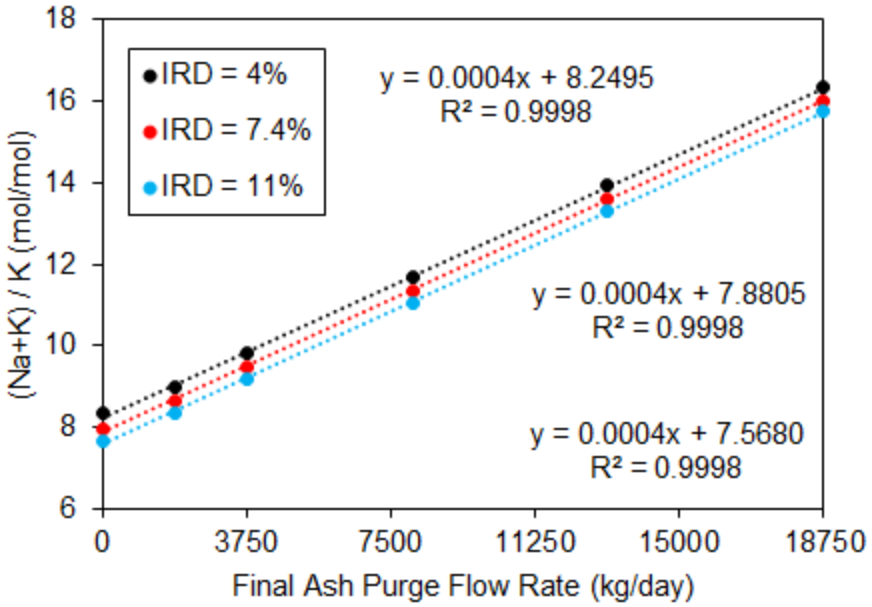

Figure 4.21: Effect of IRD on the inverse steady-state K concentration of ash at various ash purge flow rates.

4.4.4 Additional Validation of the CADSIM Model

The CADSIM model was additionally tested by attempting to reproduce the results found in literature. To test this, the CADSIM model had conditions similar to those used by Saturnino (2012) applied to it. Here, the author considered a hypothetical mill producing 1000 tons of pulp/day with no Cl and K initially in the process. The author also assumed that the amount of ash produced was 8% of the as-fired liquor dissolved solid, the EF_K was 1.5, and the EF_{Cl} was 2.5.

In order to test this, the operating conditions of the CADSIM model were adjusted to match those used by Saturnino (2012). All flow rates were scaled up to simulate a hypothetical mill capable of producing 1000 tons of pulp/day, and the process volumes were scaled to match the

conditions similar to those used by Saturnino (2012). The model was initially run with no ash being purged and no K nor Cl entering the process until a steady-state concentration was established. Then, inlet K and Cl concentrations of 1 kg/ton of pulp produced were applied (defined as t=0). After some time, purge flow rates of 5%, 10%, and 25% were separately simulated. Subsequently, the amount of purge was reduced back to 0 kg/day. The results from this test, Figure 4.22, validates that the CADSIM model from this work can reproduce results found in literature.

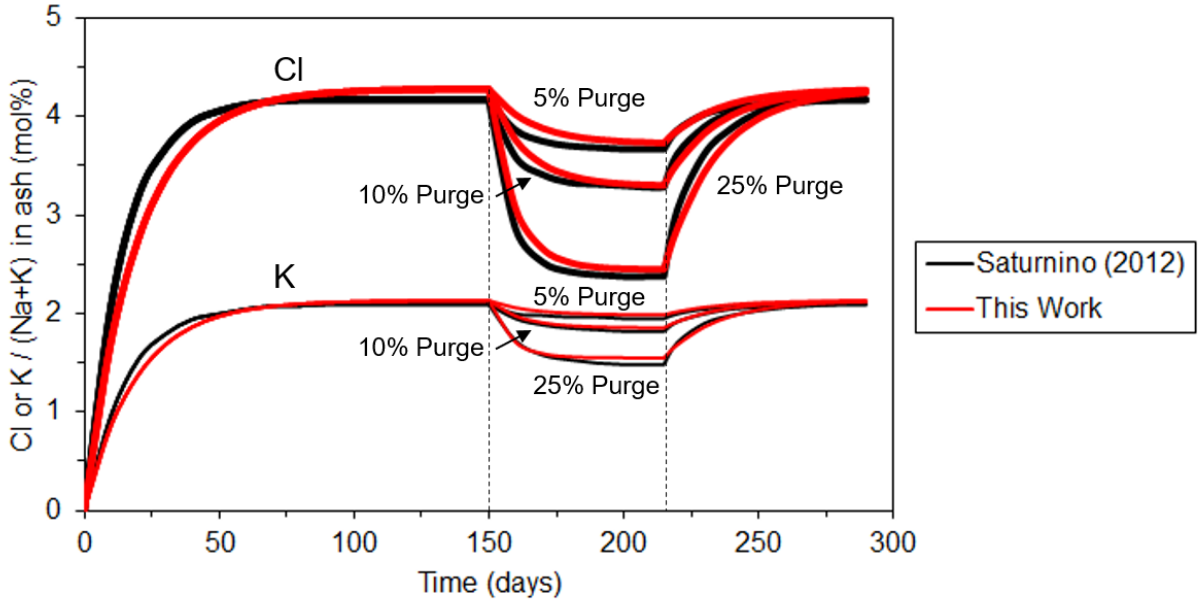

Figure 4.22: Further validation of CADSIM model to available data in literature.

4.5 Simple CSTR Mathematical Model

In order to find the general equation which describes this process, as shown previously in Figure 3.11, mass balances were needed at various locations: at the mixing of the inlet stream *f* and recycle stream *j*, around the vessel, around the concentrator, and around the entire process.

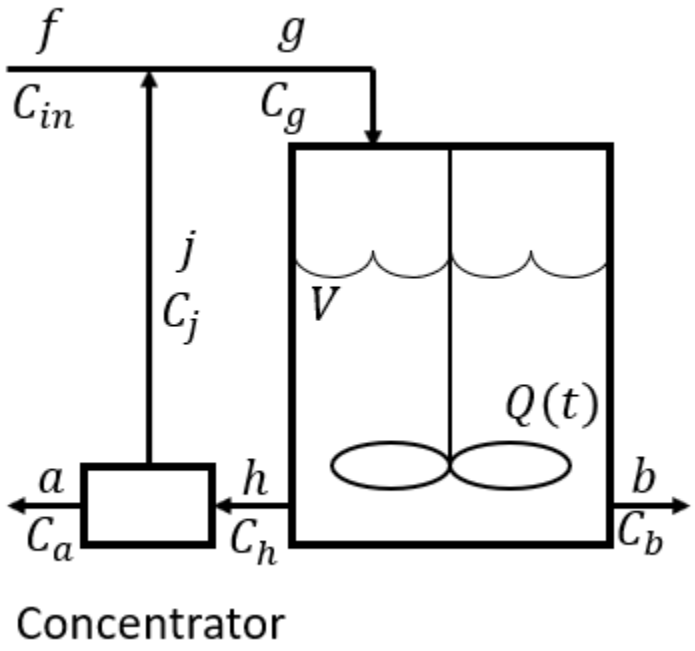

Figure 3.11: Schematic diagram of CSTR model in this work.

From a mass balance around the mixing of the inlet stream *f* and recycle stream *j*, the flow rate into the vessel, *g*, was found first. By assuming there is ideal mixing and that the density is uniform throughout the process, it can be found as the sum of the flow rates *f* and *j*, Equation 4.3. The amount flowing into the vessel, gC_g, can similarly be found by the sum of the amounts flowing in fC_{in} and jC_j, Equation 4.4.

$$g = f + j \qquad \textbf{(Eq 4.3)}$$

$$gC_g = fC_{in} + jC_j \qquad \textbf{(Eq 4.4)}$$

Applying a mass balance around the vessel, the change in the amount in the vessel over time, dQ/dt, can be found next. It is the difference between the amount flowing into the vessel, gC_g, and the amounts flowing out of the vessel, bC_b and hC_h. Assuming that the vessel is "well-mixed", the concentrations of the streams leaving the vessel, C_b and C_h, would be identical and equal to the concentration of the vessel. This concentration is the amount in the vessel at a given time, $Q(t)$, divided by the volume of the vessel, V.

$$\frac{dQ}{dt} = gC_g - b\frac{Q}{V} - h\frac{Q}{V} \qquad \textbf{(Eq 4.5)}$$

From a mass balance around the concentrator, the flow rate of the recycle stream, j, can be found as the difference between the flow rate out of the vessel, h, and the purge stream, a, Equation 4.6. Since the purge stream is concentrated, the amount that the purge stream, C_a, is concentrated from the outlet of the vessel, C_h, has to be defined. It is represented as some constant value multiple (represented as β) of the vessel outlet, Equation 4.7. Lastly, the amount flowing in the recycle stream, jC_j, can be found similarly to the flow rate of j: as the difference between the amount flowing out of the vessel, hC_h, and the amount flowing with the purge stream, aC_a. By using Equation 4.7 and the same assumption that was applied to Equation 4.5, the latter of these terms becomes $a\beta C_h$ or as shown in Equation 4.8,

$$j = h - a \qquad \textbf{(Eq 4.6)}$$

$$C_a = \beta C_h = \beta\frac{Q}{V} \qquad \textbf{(Eq 4.7)}$$

$$jC_j = h\frac{Q}{V} - a\beta\frac{Q}{V} \qquad \textbf{(Eq 4.8)}$$

Finally, applying a mass balance to the overall system and assuming the volume of the vessel remains constant, the flow rate of *b* can be found as the difference between the inlet flow rate, *f*, and the purge flow rate, *a*.

$$b = f - a \qquad \textbf{(Eq 4.9)}$$

By substitution of Equation 4.4 into Equation 4.5,

$$\frac{dQ}{dt} = fC_{in} + jC_j - b\frac{Q}{V} - h\frac{Q}{V} \qquad \textbf{(Eq 4.10)}$$

Subsequent substitution of Equation 4.8 into Equation 4.10,

$$\frac{dQ}{dt} = fC_{in} - a\beta\frac{Q}{V} - b\frac{Q}{V} \qquad \textbf{(Eq 4.11)}$$

Lastly, substituting Equation 4.9 into Equation 4.11,

$$\frac{dQ}{dt} = fC_{in} - f\frac{Q}{V} - (\beta - 1)a\frac{Q}{V} \qquad \textbf{(Eq 4.12)}$$

By factoring the term *-f/V* from the right side of Equation 4.12,

$$\frac{dQ}{dt} = -\frac{f}{V}\left(Q + (\beta - 1)\frac{a}{f}Q - VC_{in}\right) \qquad \textbf{(Eq 4.13)}$$

Separating the *Q* terms in Equation 4.13 with *dQ* and the rest with *dt*,

$$\frac{dQ}{\left(1+(\beta-1)\frac{a}{f}\right)Q - VC_{in}} = -\frac{f}{V}dt \qquad \textbf{(Eq 4.14)}$$

If the parenthesis term in Equation 4.14 is represented by a single variable, *γ*, as shown in Equation 4.15, then by integrating the left side of Equation 4.14 with respect to *Q* and the right side with respect to *t*,

$$\gamma = 1 + (\beta - 1)\frac{a}{f} \qquad \textbf{(Eq 4.15)}$$

$$\frac{1}{\gamma}\ln\left(Q-\frac{VC_{in}}{\gamma}\right)=-\frac{f}{V}t+K \qquad \textbf{(Eq 4.16)}$$

The resulting constant of integration, *K*, can be found by simplifying Equation 4.16 and taking the exponential of both sides of the equation.

$$Q-\frac{VC_{in}}{\gamma}=e^{-\gamma\frac{f}{V}t}e^{\gamma K} \qquad \textbf{(Eq 4.17)}$$

Since the initial amount in the vessel, Q_o, is known at t=0, this can be substituted into Equation 4.17.

$$Q_o-\frac{VC_{in}}{\gamma}=e^{\gamma K} \qquad \textbf{(Eq 4.18)}$$

Substitution of Equation 4.18 into Equation 4.17,

$$Q-\frac{VC_{in}}{\gamma}=e^{-\gamma\frac{f}{V}t}\left(Q_o-\frac{VC_{in}}{\gamma}\right)$$

$$Q=\frac{VC_{in}}{\gamma}+Q_oe^{-\gamma\frac{f}{V}t}-\frac{VC_{in}}{\gamma}e^{-\gamma\frac{f}{V}t}$$

$$Q=\frac{VC_{in}}{\gamma}\left(1-e^{-\gamma\frac{f}{V}t}\right)+Q_oe^{-\gamma\frac{f}{V}t} \qquad \textbf{(Eq 4.19)}$$

Given that the concentration at any time was defined as the amount at any given time, *Q(t)*, divided by the volume of the vessel, *V*, and that the initial amount is Q_o, then dividing both sides of Equation 4.19 by *V* and substituting Equation 4.15 in for γ yields,

$$C=\frac{fC_{in}}{f+(\beta-1)a}\left(1-e^{-\frac{f+(\beta-1)a}{V}t}\right)+C_oe^{-\frac{f+(\beta-1)a}{V}t} \qquad \textbf{(Eq 4.20)}$$

Looking at Equation 4.20, it can be seen that in the case when there is no purge (a=0), or when the concentration of the purge stream is equal to the concentration of the vessel (β=1), the equation

can be simplified to Equation 3.4, which is the result obtained by Saturnino (2012). Further analysis of Equation 4.20 was done to explain results obtained from the CADSIM model.

4.5.1 Evaluation of the Model at Steady-State

It was mentioned previously for Equation 3.4 that if sufficient time has passed, then the concentration is equal to C_{in}. This is a result of evaluating Equation 3.4 as $t \rightarrow \infty$, which can be seen in Equation 4.21. Since $e^{-\infty}=0$,

$$C(\infty) = C_{in}(1 - e^{-\infty}) + C_o e^{-\infty}$$

$$C(\infty) = C_{in} \qquad \textbf{(Eq 4.21)}$$

By similar analysis of Equation 4.20, evaluating as $t \rightarrow \infty$,

$$C(\infty) = \frac{fC_{in}}{f+(\beta-1)a}(1 - e^{-\infty}) + C_o e^{-\infty}$$

$$C(\infty) = \frac{fC_{in}}{f+(\beta-1)a} \qquad \textbf{(Eq 4.22)}$$

Since C is the concentration in the vessel, Equation 4.22 can be multiplied by β to define the concentration in the purge stream. Furthermore, taking the inverse of this concentration results in the following:

$$\frac{1}{\beta C(\infty)} = \frac{f+(\beta-1)a}{f\beta C_{in}} \qquad \textbf{(Eq 4.23)}$$

Looking at Equation 4.23, the inverse of the steady-state concentration is predicted to be linear with respect to the purge flow rate, a. A plot of the inverse steady-state ash concentration versus the ash purge flow rate from the CADSIM model was previously shown in Figure 4.20. Looking

at Figure 4.20, it can be seen that for both K and Cl linear trends, with R^2 values nearly equal to 1, are produced with respect to the ash purge flow rate. Furthermore, the trend for Cl, which has a larger enrichment factor than K, has a slope which is also larger than that of the trend for K. This is the predicted result for a larger value of β in Equation 4.23. Lastly, the inlet concentration of K is larger than that of Cl's; also, the resulting intercept of the K trend is less than the intercept of the Cl trend. This is once again predicted in Equation 4.23 for a larger value of C_{in}.

However, looking at Figure 4.21, which shows the effect of IRD on the previously described lines for K, it can be seen that the changes to the IRD results in vertical translations of the resulting lines. Looking at Equation 4.20, there is no such effect predicted by the internal recycle streams *h* or *j*.

In summary, this mathematical model is able to describe the results of the effect of ash purge flow rate on the steady-state ash concentrations, but it is unable to describe the resulting effect of IRD on these steady-state ash concentrations predicted by the CADSIM model.

4.5.2 Evaluation of the Time Constant

It was mentioned previously for Equation 3.4 that the time needed to reach steady-state was dependant on the ratio *f/V*. This is a result of comparing the general first order process, as previously shown in Equation 4.1, to a similarly arranged first term of Equation 3.4. This arranged term is shown in Equation 4.24.

$$C = C_{in}\left(1 - e^{\left(-\frac{f}{V}t\right)}\right) \qquad \textbf{(Eq 4.24)}$$

By directly comparing the exponential exponents,

$$\frac{1}{\tau} = \frac{f}{V} \qquad \textbf{(Eq 4.25)}$$

Recalling that τ is the process time constant, Equation 4.25 shows that the process time constant is directly proportional to *V* and inversely proportional to *f*. This can also be stated as the inverse of the process time constant being equal to the ratio *f/V*.

A similar evaluation can be done for Equation 4.20, by comparing its first term of the equation to the general first order process. Arranging the first term of Equation 4.20,

$$C = \frac{fC_{in}}{f+(\beta-1)a}\left(1 - e^{-\frac{f+(\beta-1)a}{V}t}\right) \qquad \textbf{(Eq 4.26)}$$

By direct comparison of the exponential exponents of Equation 4.1 and Equation 4.26,

$$\frac{1}{\tau} = \frac{f+(\beta-1)a}{V} \qquad \textbf{(Eq 4.27)}$$

Looking at Equation 4.27, the inverse of the process time constant is predicted, again, to be a linear function with respect to the purge flow rate, *a*. A plot of the inverse of the process time constant versus the ash purge flow rate from the CADSIM model was previously shown in Figure 4.18. Looking at Figure 4.18, linear trends for both K and Cl, with R^2 values nearly equal to 1, are produced with respect to the ash purge flow rate. Furthermore, the trend for Cl, which has a larger enrichment factor than K, has a slope which is larger than that of K's. This is predicted in Equation 4.27 for a larger value of *β*. Lastly, the intercepts for both K and Cl are nearly identical, which is also predicted in Equation 4.27 for an *a* value of zero.

5. Conclusions

An analysis and investigation into the unusual Cl trend that was observed in the ESP ash of a Canadian mill was conducted. The following was observed:

- The trend of the Cl content of the ESP ash was determined to follow a simple apparent cyclical trend. This trend has a period of approximately 360 days and has lasted at least 5 years. During the most recent cycle, a 90-day duration deviated from this otherwise predicable trend. An investigation into this duration found no evidence in available mill data nor from insight provided by mill personnel which could explain this trend.
- Several process variables which are found in literature, that are known to either affect enrichment factors of ESP ash or to control the Cl content in the liquor cycle, were analyzed. However, no trends of their measured data recorded by the mill were capable of explaining the cyclical trend observed in the Cl content of the ash nor the resulting EF_{Cl} trend obtained during the sampling period.
- A gap in knowledge relating to the concentration of Cl in ESP ash has been identified. Current literature failed to explain the unusual trend of Cl concentration found in the ESP ash in this operating recovery boiler.

A CADSIM model was created to simulate the K and Cl concentrations in the liquor cycle and subsequently in the ESP ash for this mill. In summary,

- A model output (representing the loss to grits, dregs, liquor spills, etc.) was tuned for K to match available liquor cycle data during a calibration period. Validation of the model was done by simulating the K in ESP for an extended period of time and comparing the results to available mill data. A sensitivity analysis using different K input concentrations was

tested. From the validations of these analyses, near-equivalent results were obtained. It was determined that the CADSIM model is capable of reproducing K trends observed in the mill data.

- Tuning of the Cl output was unable to match available liquor cycle data during the calibration period. Consequently, the proportionality constant was unable to be obtained for Cl and was, as a result, assumed to be equal to that of the value obtained for K. Using this value, a trend of missing Cl input during the calibration period was determined. However, no trends were able to be meaningfully extrapolated to periods outside of this duration; for that reason, no additional Cl input was considered. The simulation of Cl in the ESP ash that followed during the validation period was unable to reproduce the trend observed in the mill data of Cl for a single EF_{Cl} value used. Nevertheless, a hypothetical trend of EF_{Cl} values needed to reproduce the mill data was determined. This hypothetical trend was consistent with the EF_{Cl} values determined from black liquor and ESP ash samples obtained during the sampling period.
- The model's response to a step change in the ash purge flow rate, under constant input, was studied. This response was found to follow a first order response. A numerical approach to determine the time constant of the system, τ, was established using Excel, and an acceptable steady-state concentration was determined to be obtained after 4.6 τ. It was found that τ decreased as the purge flow rate increased and that the trend of the τ decreased quicker for Cl than it did for K. The trend of the ESP ash concentration was also found to decrease with ash purge flow rate; this result is consistent with results previously found in literature. The effect of IRD on the concentration in ESP ash was also determined.

Lastly, a simplified mathematical model of a kraft liquor cycle was derived to explain results obtained from the CADSIM model. In particular,

- The trends for the inverse of the steady-state ash concentrations were determined to be linear with respect to ash purge flow rate. These trends have R^2 values close to 1. The slopes and intercepts of these lines were found to be directly influenced by the inlet concentration, inlet flow rates, and enrichment factors.
- The trends for the inverse of the process time constants, τ, were also determined to be linear with respect to ash purge flow rate. Once again, these trends have R^2 values close to 1. The intercepts were found to be nearly identical for both K and Cl. Meanwhile, the slopes of these lines were found to be directly influenced by enrichment factors.
- The mathematical model was unable to explain the effect of the IRD on the steady-state concentrations of the ash observed in the CADSIM model.

5.1 Recommendation for Mill Operations

From this work, several recommendations for the mill have been identified in current operations:

- Switching the grade of caustic from diaphragm grade to a low-Cl membrane grade proved ineffective at reducing the trend found in the Cl concentrations of ESP ash.
- More aggressive ESP ash purging strategies that are currently employed by the mill are not found to prevent the high Cl concentrations observed in the ESP ash.
- Investigations into operating procedures and the liquor cycle should be conducted to identify potential sources of significant Cl input to the liquor cycle that are not currently considered.

- Further testing of black liquor samples, such as the combustion in a Laminar Entrained-Flow Reactor (LEFR), should be done to identify if the trends of Cl concentration and EF_{Cl} observed in the ESP ash can be reproduced in a lab setting.

5.2 Recommendation for Future Work

In this work, a gap in knowledge was identified affecting the Cl concentration in ESP ash. It is suggested that several samples of liquor should be analyzed and combusted in a laboratory environment to reproduce these trends of Cl concentration and EF_{Cl} found in the ESP ash in a controlled setting. At that time, further investigation can be conducted to bridge the gap in knowledge that was identified in literature by this work.

6. References

Andersson, P. (2014). *A dynamic Na/S balance of a kraft pulp mill* [Master's Thesis, Karlstad University].

Aurel Systems. (n.d.). *Products – CADSIM Plus*. Retrieved from https://www.aurelsystems.com/cadsim-plus/, accessed 2022.

Bialik, M., Jensen, A., & Ahlroth, M. (2015). New challenges regarding nonprocess elements in the liquor and lime cycle. *TAPPI, 14*(7), 421 – 429.

Brännvall, E. (2009). Overview of Pulp and Paper Processes. In M. Ek et al. (Eds), *Pulp and Paper Chemistry and Technology Volume 2* (pp. 1-11). Walter de Gruyter.

Brink, J. (2021). *The effect of black liquor droplet in-flight time on kraft recovery boiler dust formation* [Master's Thesis, Åbo Akademi University].

Burazin, M. (1986). *A Dynamic Model of Kraft-Anthraquinone Pulping* [Doctoral Dissertation, Lawrence University].

Chakar, F. & Ragauskas, A. (2004). Review of current and future softwood kraft lignin process chemistry. *Industrial Crops and Products, 20*, 131-141.

Deshwal, B. & Lee, H. (2005). Manufacture of Chlorine Dioxide from Sodium Chlorate: State of the Art. *Journal of Industrial and Engineering Chemistry, 11*(3), 330-346.

ERCO Worldwide. (n.d.). *ClO_2 Pulp Bleaching Technologies*. Retrieved from https://www.ercoworldwide.com/our-products/technical-services/clo2-technologies/?locale=en, accessed 2022.

Frederick, W. J., Vakkilainen, E., & Dent, G. (1998). Effects of Temperature and SO2 on Chloride and Potassium Enrichment Factors in Kraft Recovery Boilers. *International Chemical Recovery Conference Proceedings*.

Gellerstedt, G. (2009). Chemistry of Chemical Pulping. In M. Ek et al. (Eds), *Pulp and Paper Chemistry and Technology Volume 2* (pp. 92-108). Walter de Gruyter.

Guimarães, M., Tran, H., & Cardoso, M. (2014). A novel method for determining the internal recycled dust load in kraft recovery boilers. *TAPPI, 13*(8), 27-33.

Hach. (2014). *Tetraphenylborate Method* (Method 8049/DOC316.53.01339). Hach. https://www.hach.com/p-potassium-reagent-set/2459100.

Hach. (2018). *Mercuric Thiocyanate Method* (Method 8113/DOC316.53.01017). Hach. https://ca.hach.com/chloride-reagent-set-mercuric-thiocyanate/product-downloads?id=14533957039.

Henricson, K. (2005). *Chemical Recovery Cycle*.

Hupa, M. (2007). Recovery Boiler Chemical Principles. *TAPPI Kraft Recovery Course 2007, 2*.

Hupa M. & Frederick, W. J. (2007) Combustion of Black Liquor Droplets. *TAPPI Kraft Recovery Course 2007, 1*.

Isaak, P., Tran, H., Barham, D., & Reeve, D. (1986). Stickiness of Fireside Deposits in Kraft Recovery Units. *Journal of Pulp and Paper Science, 12*(3), 84-88.

Jokiniemi, J., Pyykönen, J., Mikkanen, P., & Kauppinen, E. (1996). Modeling fume formation and deposition in kraft recovery boilers. *TAPPI, 17*(7), 171-181.

Jones, A., Tran, H., Vakkilainen, E., & Salmenoja, K. (2015). Chloride and potassium measurement and control in the pulping and chemical recovery cycle. *TAPPI TIP 0416-15.*

Karlemo, C. (2019). *Non-process elements in the recovery cycle of six Finnish Kraft pulp mills* [Master's Thesis, Åbo Akademi University].

Khalaj-Zadeh, A. (2008). *A Study of the Composition of Carryover Particles in Kraft Recovery Boilers* [Doctoral Dissertation, University of Toronto].

Koch, G. (2006). Raw Material for Pulp. In H. Sixta (Ed), *Handbook of Pulp Volume 1* (pp. 21-68). Wiley-VCH.

Kochesfahani, S. H. (1999). *Particulate Formation During Black Liquor Char Bed Burning* [Doctoral Dissertation, University of Toronto].

Leppänen, A., Tran, H., Välimäki, E., & Oksanen, A. (2014). Modelling Fume Deposit Growth in Recovery Boilers: Effect of Flue Gas and Deposit Temperature. *Journal of Science & Technology for Forest Products and Processes, 4*(1), 50-57.

Lundström, J. (2007). *Chloride and potassium balances in the future energy efficient pulp mills* [Master's Thesis, Royal Institute of Technology].

Mäkitalo, M., Maurice, C., Jia, Y., & Öhlander, B. (2014). Characterization of Green Liquor Dregs, Potentially Useful for Prevention of the Formation of Acid Rock Drainage. *Journal of Minerals, 4*, 330-344.

Manskinen, K., Nurmesniemi, H., & Pöykiö, R. (2010). Total and extractable non-process elements in green liquor dregs from the chemical recovery circuit of a semi-chemical pulp mill. *Chemical Engineering Journal, 166*, 954-961.

Martins, F., Martins, J., Farracin, L., & Cunha, C. (2007). Mineral phases of green liquor dregs, slaker grits, lime mud and wood ash of a Kraft pulp and paper mill. *Journal of Hazardous Materials*, 1-8.

Mehtonen, N. (2013). Literature Study of Present and New Methods for Reducing Non-Process Elements in the Lime Circulation of a Kraft Pulp Mill [Master's Thesis, Aalto University].

Miliander, L. (2009). Pulp Washing. In M. Ek et al. (Eds), *Pulp and Paper Chemistry and Technology Volume 2* (pp. 165-187). Walter de Gruyter.

Öhman, F. & Delin, L. (2014). *Electrolysis of sodium sulphate – efficient use of saltcake and ESP dust in pulp mills*.

Old World Industries, LLC. (2016). *Diaphragm Grade 50% Liquid Caustic Soda: Product Specification CAS# 1310-73-2*. Retrieved from http://www.owichloralkali.com/Portals/0/Documents/OWIC%20Spec%20Diaphragm.pdf , accessed 2022.

OxyChem. (2022). *Caustic Soda Handbook*. Retrieved from https://www.oxy.com/globalassets/documents/chemicals/products/chlor-alkali/caustic.pdf, accessed 2022.

Pfromm, P. (1999). *Chloride and Potassium in the Kraft Recovery Cycle: A Practical Guide*.

Quina, M. & Pinheiro, C. (2020). Inorganic Waste Generated in Kraft Pulp Mills: The Transition from Landfill to Industrial Applications. *Journal of Applied Sciences, 10*(7), 1-20.

Reis, V., Frederick, W. J., Wåg, K., Iisa, K., & Sinquefield, S. (1995). Effects of temperature and oxygen concentration on potassium and chloride enrichment during black-liquor combustion. *TAPPI, 78*(12), 67-76.

Resolute Forest Products. (n.d.). *Operations – Thunder Bay*. Retrieved from https://www.resolutefp.com/installation_site.aspx?siteid=135&langtype=4105, accessed 2022.

Salmenoja, K., Poukka, O., & Battegazorre, M. (2009). *Management of Non-Process Elements in Eucalyptus Kraft Pulp Mills*.

Sanchez, D. (2007). Recausticizing – Principles and Practice. *TAPPI Kraft Recovery Course 2007, 1*.

Santos, R. and Hart, P. (2014). Brownstock washing – A review of the literature, *TAPPI, 13*(1), 9-19.

Saturnino, D. (2012). *Modeling of Kraft Mill Chemical Balance* [Doctoral Dissertation, University of Toronto].

Svensson, J. (2012). *Non-process Elements in the Green Liquor System*.

Swanda, A., Seborg, D., Holman, K., & Sweerus, N. (1997). Dynamic models of the causticizing process. *TAPPI, 80* (12), 123-134.

TAPPI. (1999). *Solids content of black liquor* (T 650 om-99). TAPPI. https://www.tappi.org/.

TAPPI. (2000). *Analysis of pulping liquors by suppressed ion chromatography* (T 699 om-00). TAPPI. https://www.tappi.org/.

Taylor, K. & McGuffie, B. (2007). Investigation of non-process element chemistry at Elk Falls mill – green liquor clarifier and lime cycle. *Pulp & Paper Canada, 108*(2), 27-32.

Theliander, H. (2009a). Recovery of Cooking Chemicals: the Treatment and Burning of Black Liquor. In M. Ek et al. (Eds), *Pulp and Paper Chemistry and Technology Volume 2* (pp. 297-323). Walter de Gruyter.

Theliander, H. (2009b). The Recovery of Cooking Chemicals: the White Liquor Preparation Plant. In M. Ek et al. (Eds), *Pulp and Paper Chemistry and Technology Volume 2* (pp. 297-323). Walter de Gruyter.

Tran, H. (1986). How does a kraft recovery boiler become plugged? *TAPPI, 69*(11), 102-106.

Tran, H., Barham, D., & Reeve, D. (1990). Chloride and potassium in the kraft chemical recovery cycle. *Pulp & Paper Canada, 91*(5), 185-190.

Tran, H. & Earl, P. (2004). Chloride and Potassium Removal Processes for Kraft Pulp Mills: A Technical Review. *International Chemical Recovery Conference*.

Tran, H. (2007a). Lime Kiln Chemistry and Effects on Kiln Operations. *TAPPI Kraft Recovery Course 2007, 1*.

Tran, H. (2007b). Recovery Boiler Fireside Deposits and Plugging Prevention. *TAPPI Kraft Recovery Course 2007, 2*.

Tran, H. & Vakkilainen, E. (2007). The Kraft Chemical Recovery Process. *TAPPI Kraft Recovery Course 2007, 1*.

Ulmgren, P. (1997). Non-process elements in a bleached kraft pulp mill with a high degree of system closure – state of the art. *Nordic Pulp and Paper Research Journal, 111997*.

Vakkilainen, E. (2006). *Kraft recovery boilers – High dry solids firing*.

Vakkilainen, E. (2010). *Predicting ash properties in recovery boilers*.

Wessel, R., Baxter, L., Shaddix, C., Verrill, C., Frederick, W. J., Lien, S., & Tran, H. (2004). *Particle Formation And Deposition In Recovery Boilers*.

Wessel, R. (2007). Black Liquor Spraying. *TAPPI Kraft Recovery Course 2007, 2*.

Westlake Chemical. (2022). *Product Specifications: 50% Caustic Soda Membrane Grade*. Retrieved from https://www.westlake.com/sites/default/files/Liquid%20Caustic%20Soda%2050%25%20Membrane%20Grade.pdf, accessed 2022.

7. Appendices

Appendix A – Recovery Boiler Trends

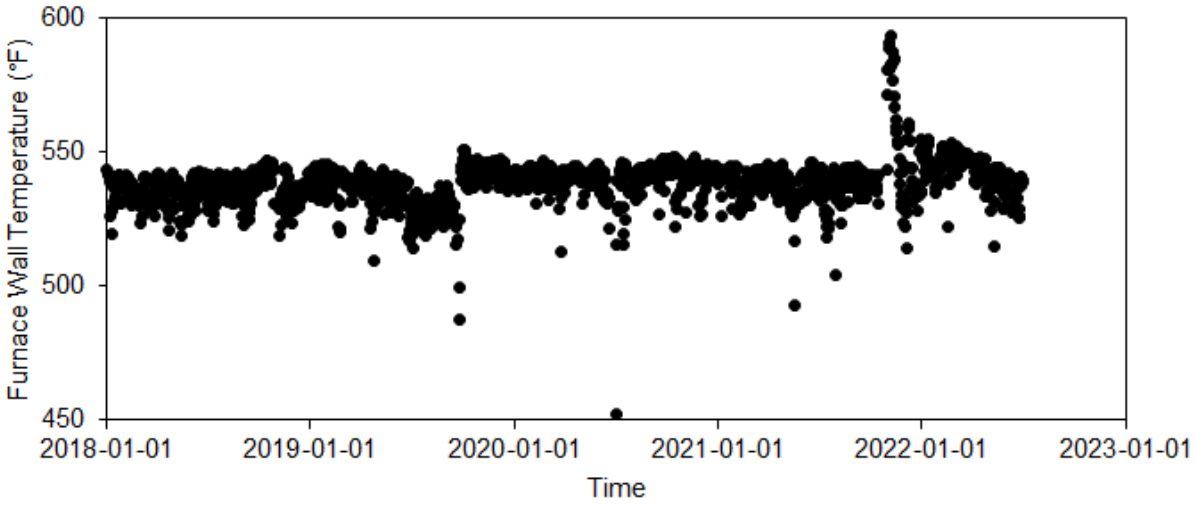

Figure A.1: Temperature of water in recovery boiler wall tubes.

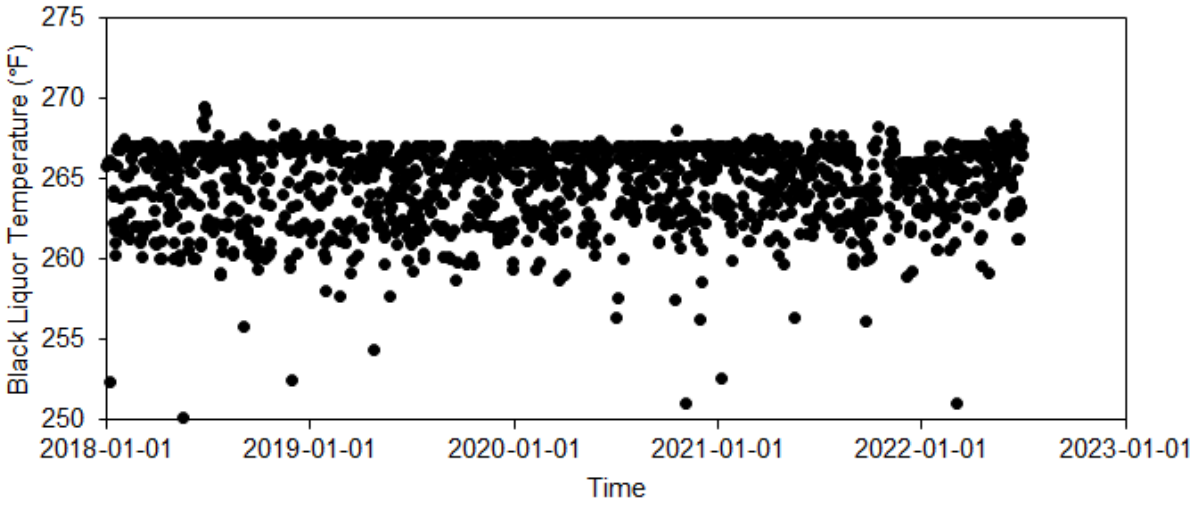

Figure A.2: Temperature of fired black liquor in recovery boiler.

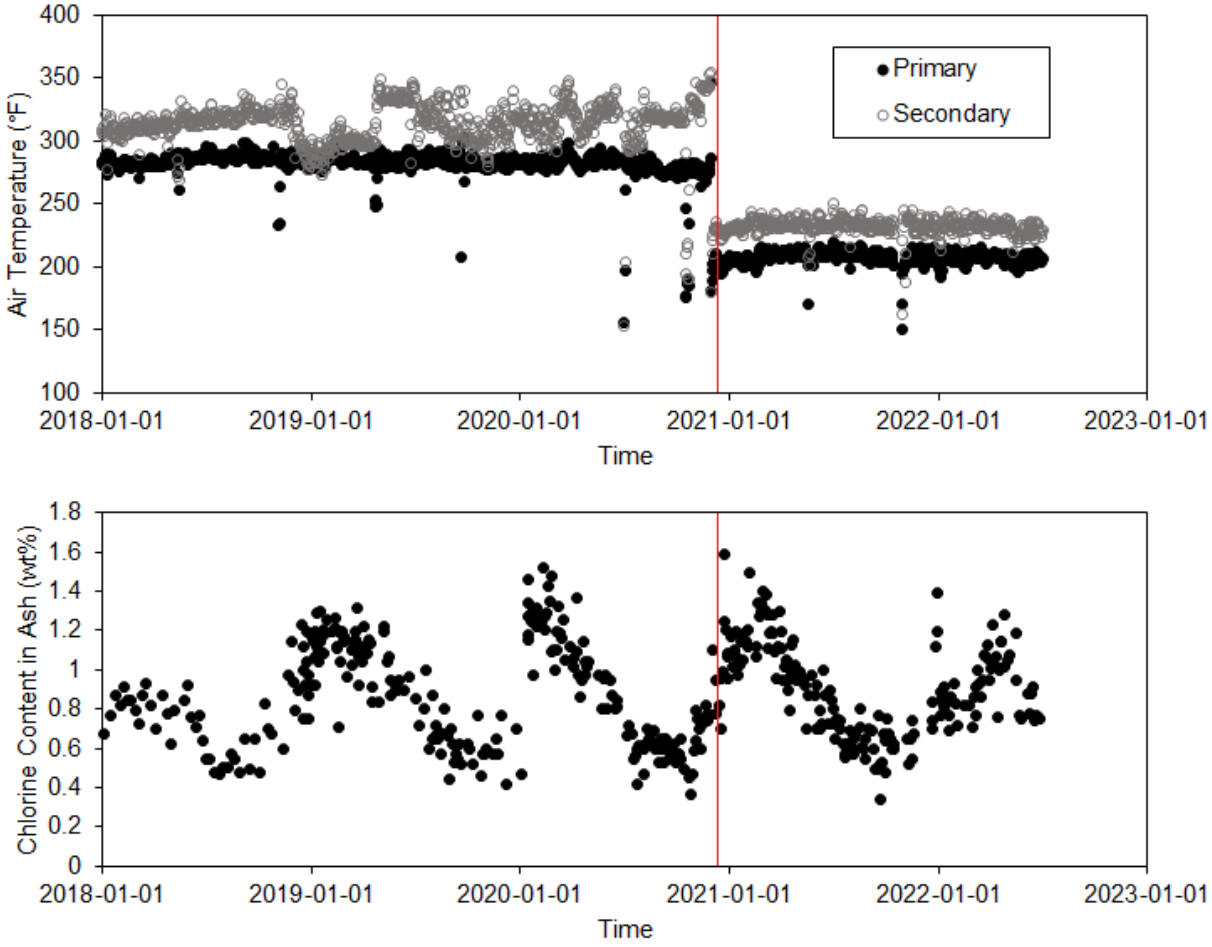

Figure A.3: Comparison of combustion air temperature (top) and Cl content in recovery boiler ash (bottom).

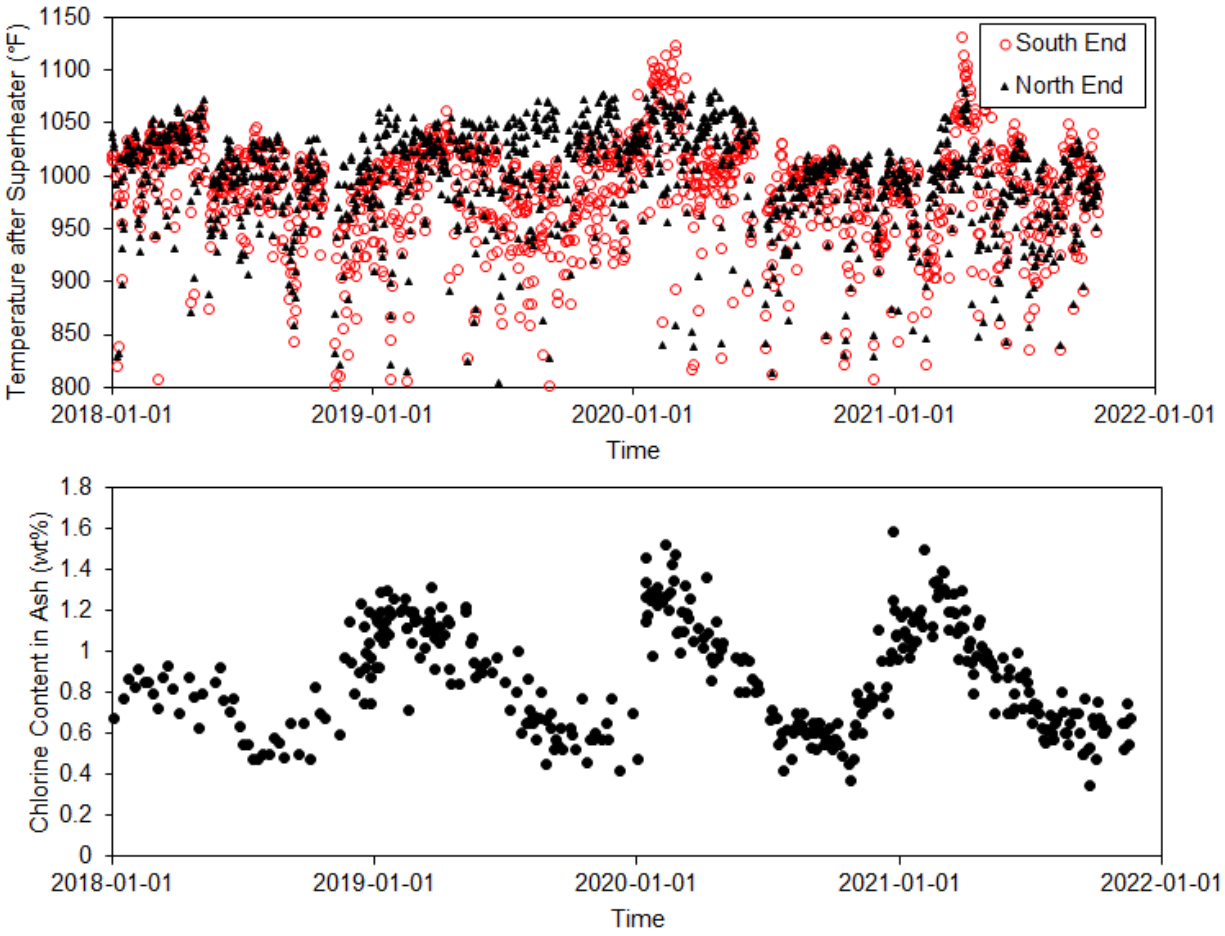

Figure A.4: Comparison of flue gas temperature after superheaters (top) and Cl content in recovery boiler ash (bottom).

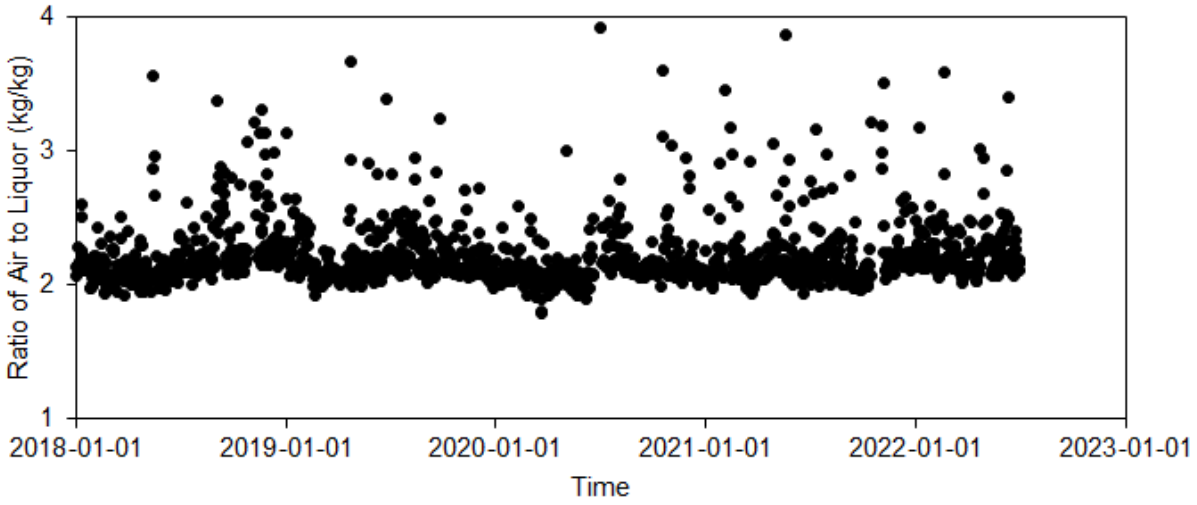

Figure A.5: Mass ratio of combustion air to black liquor in the recovery boiler.

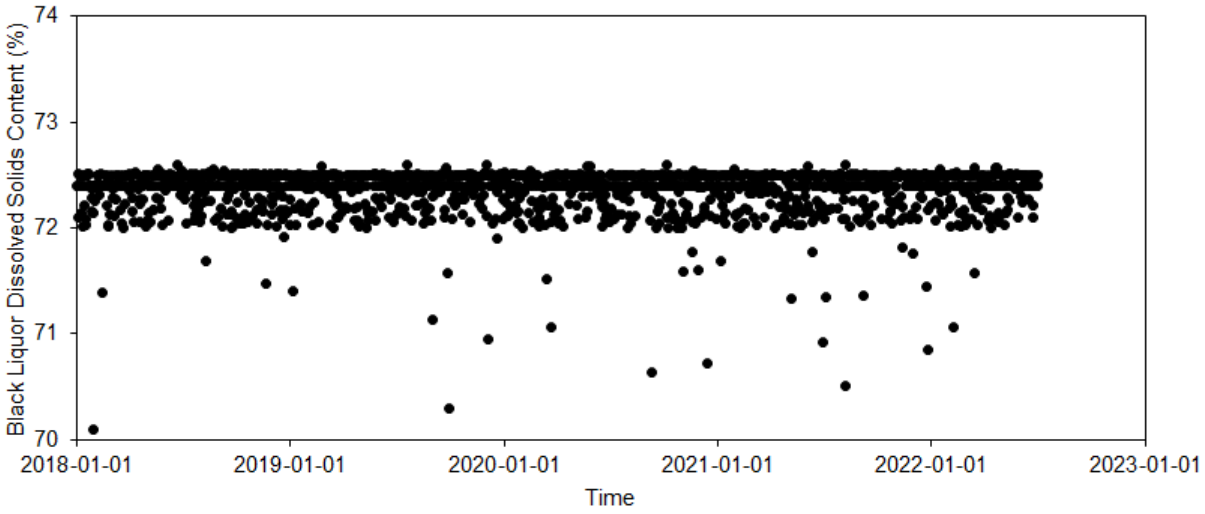

Figure A.6: Dissolved solids content of fired black liquor in the recovery boiler.

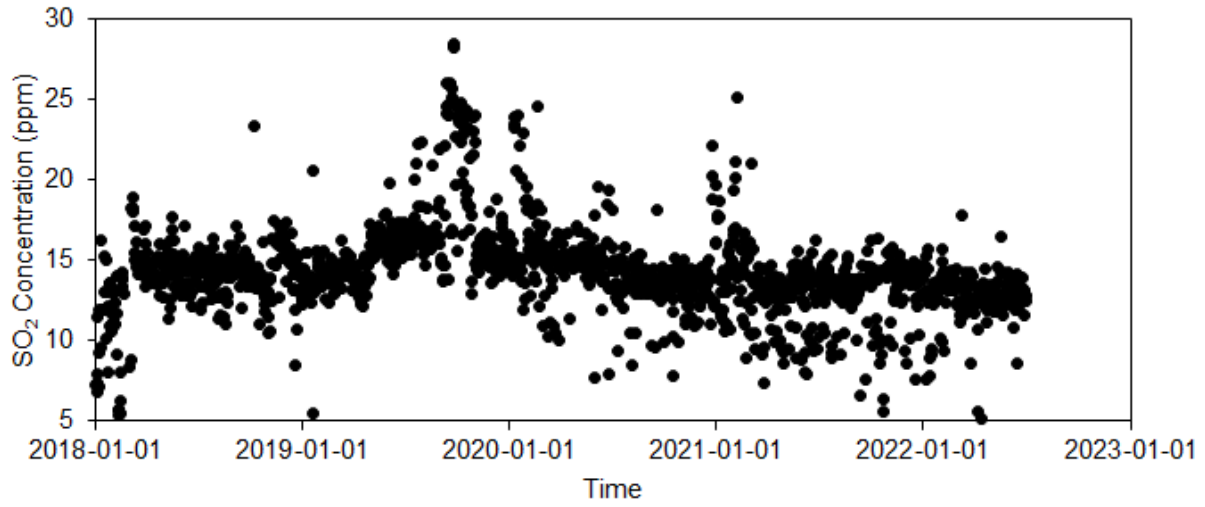

Figure A.7: SO_2 emissions from recovery boiler flue gas.

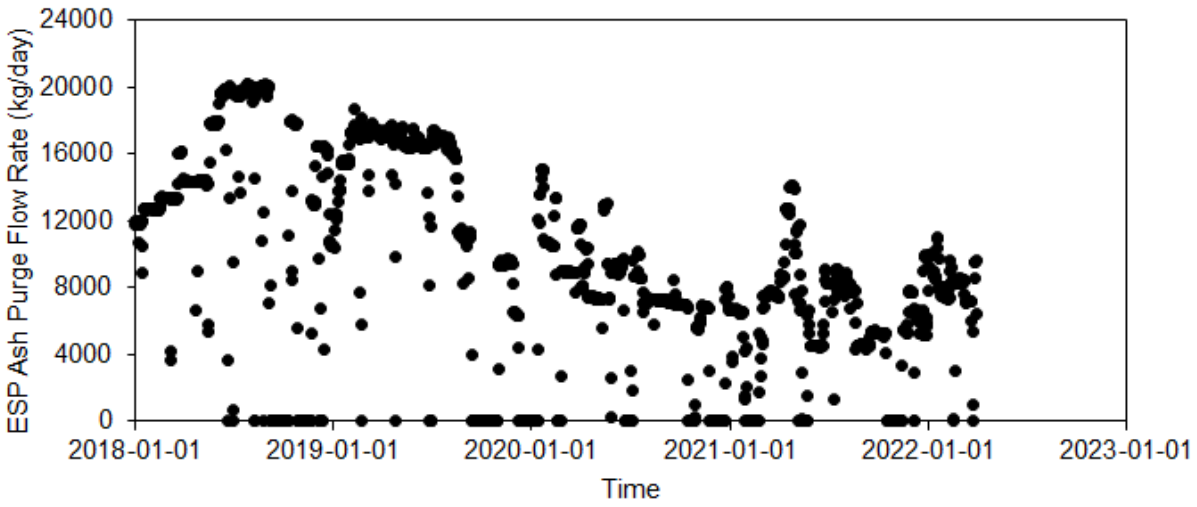

Figure A.8: Purging flow rate of ESP ash.

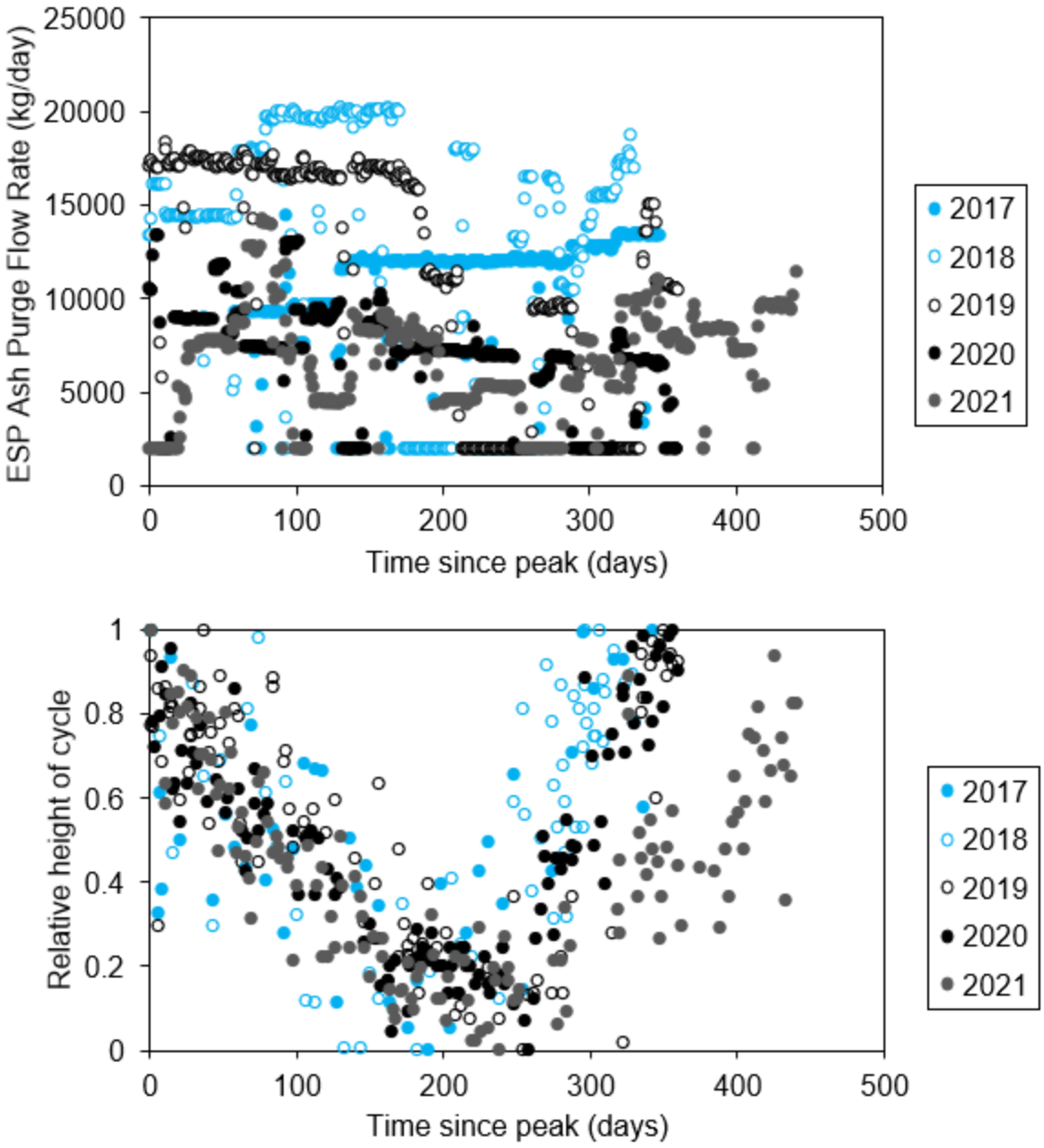

Figure A.9: Comparison of ESP ash purging flow rate (top) and normalized Cl content in ESP ash cycles (bottom).

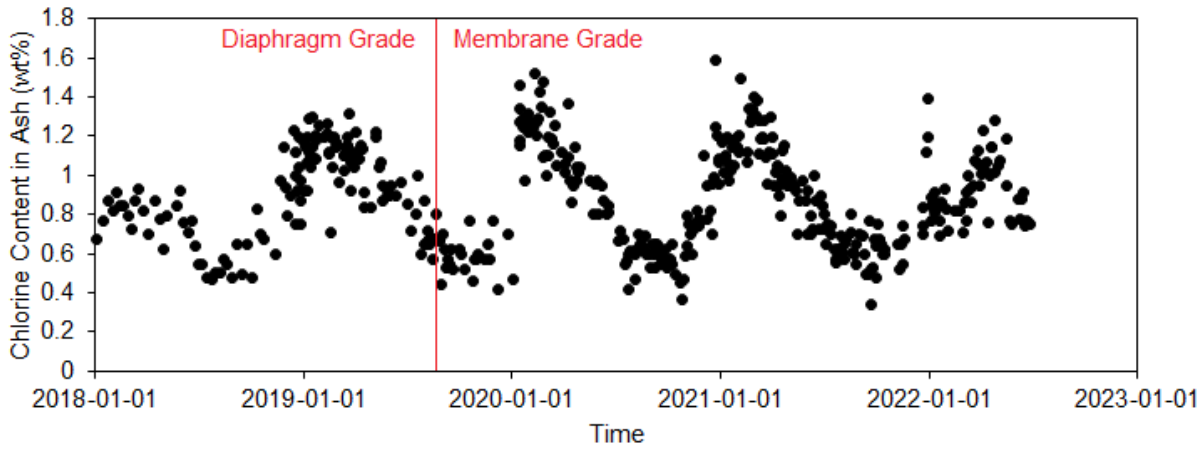

Figure A.10: Effect of caustic grade on the trend of Cl content in ESP ash.

Appendix B – Mass Balance Data

Table B.1: Available data measured by the mill used in mass analysis.

Stream/ Property	Average Value	Units
Wood		
Digester Production Rate	904.7	AD mt/ day
Water		
Pulp Washer Shower Flow Rate	3,871.5	L/ min
Temperature	120	°F
Saltcake		
R10 Generated ClO_2 Flow Rate	1,700.9	L/ min
R10 Generated ClO_2 Concentration	9.03	g/ L
R11 Consumed Chlorate	4,925.9	kg/ day
Caustic		
Flow Rate	1.799	gal/ min
Pulp		
Slurry Flow Rate	12,926	L/ min
Slurry Consistency	4.014	%
Ash		
Purge Flow Rate	10,341	kg/ day

Table B.2: Average stream compositions used in mass analysis.

Stream	Na	S	Cl	K	Units
Wood					
Hardwood	53	80	43	995	mg/ OD kg
Softwood	25	65	53	415	mg/ OD kg
Water	1.90	1.42	8.55	0.51	mg/ kg
Saltcake *	323,700	225,700	-	-	mg/ kg
Caustic **					
Diaphragm Grade	287,400	407	5,990	129	mg/ kg
Membrane Grade	287,400	9.0	68	129	mg/ kg
Pulp					
Hardwood	2,960	425	74	335	mg/ OD kg
Softwood	2,840	550	89	320	mg/ OD kg
Ash	328,400	155,500	13,850	46,010	mg/ kg
Dregs	23,150	10,040	1,090	1,850	mg/ kg
Grits	18,600	4,300	2,300	1,500	mg/ kg

* Saltcake assumed to be pure Na_2SO_4

** Caustic assumed to be 50 wt% NaOH.